Additional Applications of Transesophageal Echocardiography

16

Pierre C. Wong

Abstract

While the majority of this book addresses the use of transesophageal echocardiography (TEE) for the evaluation of patients with congenital heart disease (CHD), there are a number of other conditions in which TEE can play a significant role in pediatric and young adult patients. Some conditions, such as infective endocarditis, can occur in patients with a history of CHD. Other pathologies, such as cardiac tumors, can be seen in the absence of coexisting CHD. This chapter addresses additional applications of TEE in the pediatric and young adult population.

Keywords

Endocarditis • Bacterial • Heart valve prosthesis • Heart neoplasms • Heart-assist devices • Heart transplantation • Lung transplantation • Aneurysm • Dissecting • Echocardiography • Transesophageal

Introduction

While the majority of this book addresses the use of transesophageal echocardiography (TEE) for the evaluation of congenital heart disease (CHD), there are other conditions in which TEE can prove beneficial in pediatric and young adult patients with and without CHD. This chapter discusses some of the more common clinical scenarios in which this might occur, and how TEE can contribute useful (and sometimes invaluable) additional information. Some situations will require TEE to be performed both in and out of the intraoperative setting.

Infective Endocarditis

Infective endocarditis (IE) is defined as a microbial infection of the endocardial (endothelial) surface of the heart, primarily involving the valves but also affecting other endocardial surfaces, including any prosthetic or foreign material in the heart. Infection can also occur on the endothelial surfaces of the great vessels (including the great arteries), and in this case it is known as infective endarteritis. Infective endocarditis can be caused by a number of different organisms, mainly bacteria and fungae (Table 16.1), and the clinical course ranges in severity from indolent to fulminant [1, 2]. Despite the fact that

P.C. Wong, MD
Division of Cardiology, Children's Hospital Los Angeles, Department of Pediatrics, Keck School of Medicine, University of Southern California, 4650 Sunset Blvd, Mailstop #34, Los Angeles, CA 90027, USA
e-mail: pwong@chla.usc.edu

The online version of this chapter (doi:10.1007/978-1-84800-064-3_16) contains supplementary material, which is available to authorized users.

P.C. Wong, W.C. Miller-Hance (eds.), *Transesophageal Echocardiography for Congenital Heart Disease*,
DOI 10.1007/978-1-84800-064-3_16, © Springer-Verlag London 2014

Table 16.1 Organisms commonly associated with infectious endocarditis

Bacteria
Viridans group streptococci (alpha-hemolytic)—*S. mitis, S. sanguis, S. mutans,* etc.
Staphylococcus aureus
Coagulase-negative staphylococcus
Streptococcus pneumonia
Streptococcus bovis and other streptococci
Enterococcus species
HACEK (*Hemophilus* species, *Aggregatibacter actinomycetemcomitans, Cardiobacterium hominis, Eikinella* species, *Kingella kingae)*
Pseudomonas species
Culture negative (*Chlamydia* species, *Coxiella burnetii, Abiotrophia* species, *Bartonella* species, *Brucella* species, *Legionella* species, etc.)
Fungal
Candida albicans
Candida tropicalis
Histoplasma capsulatum
Aspergillus
Cryptococcus neoformans

Table 16.2 Modified Duke criteria: definition of terms used for the diagnosis of infective endocarditis (IE)

Major criteria
Blood culture positive for IE
Typical microorganisms consistent with IE from two separate blood cultures:
Viridans streptococci, *Streptococcus bovis,* HACEK group, *Staphylococcus aureus;* or
Community-acquired enterococci, in the absence of a primary focus; or
Microorganisms consistent with IE from persistently positive blood cultures, defined as follows:
At least two positive cultures of blood samples drawn >12 h apart; or
All of three or a majority of ≥4 separate cultures of blood (with first and last sample drawn at least 1 h apart)
Single positive blood culture for Coxiella burnetii or antiphase I IgG antibody titer >1:800
Evidence of endocardial involvement
Echocardiogram positive for IE **(TEE recommended in patients with prosthetic valves, rated at least "possible IE" by clinical criteria, or complicated IE [paravalvular abscess]; TTE as first test in other patients),** defined as follows:
Oscillating intracardiac mass on valve or supporting structures, in the path of regurgitant jets, or on implanted material in the absence of an alternative explanation; or
Abscess; or
New partial dehiscence of prosthetic valve
New valvular regurgitation (worsening or changing of pre-existing murmur not sufficient)
Minor criteria
Predisposition, predisposing heart condition or injection drug use
Fever, temperature >38 °C
Vascular phenomena, major arterial emboli, septic pulmonary infarcts, mycotic aneurysm, intracranial hemorrhage, conjunctival hemorrhages, and Janeway's lesions
Immunologic phenomena: glomerulonephritis, Osler's nodes, Roth's spots, and rheumatoid factor
Microbiological evidence: positive blood culture but does not meet a major criterion as noted above[a] or serological evidence of active infection with organism consistent with IE
Echocardiographic minor criteria eliminated

From: Li et al [9]; reproduced with permission, Oxford University Press.
(Modifications shown in boldface)
TEE transesophageal echocardiography, *TTE* transthoracic echocardiography
[a]Excludes single positive cultures for coagulase-negative staphylococci and organisms that do not cause endocarditis

IE begins as an infection of the endocardial surface, the infectious process can be highly invasive, causing extensive destruction of heart valve and surrounding tissue, as well as intramyocardial abscesses. Some of the most severe complications resulting from IE include congestive heart failure (due to valvar regurgitation), systemic and pulmonary embolic phenomena, sepsis, arrhythmias, myocardial failure, and death [3].

A number of conditions can predispose to IE, including mitral valve prolapse, rheumatic heart disease, indwelling catheters, intravenous drug abuse, prosthetic valves, and both unrepaired and repaired CHD [1]. The role of congenital cardiac disease as a predisposing factor for IE continues to increase in developed countries; CHD now appears to be the predominant underlying condition for IE in children over the age of 2 years [4]. Certain congenital heart lesions are recognized to have an association with IE, including ventricular septal defects, patent ductus arteriosus, aortic valve abnormalities, and tetralogy of Fallot [5]. Furthermore, increasing numbers of children with IE have had previous palliative or corrective surgery for CHD [4, 6]. However, IE can occur in the absence of any structural heart disease; this is seen in approximately 2–5 % of younger pediatric IE cases (2 months to 15 years of age), and 25–45 % of older IE patients (15–60 years of age) [1, 7].

Because of the variability in clinical presentation, the diagnosis of IE is not always straightforward. To assist in diagnosis, a set of criteria—known as the Duke criteria—were proposed in 1994 as a diagnostic schema for patients with suspected IE [8]. Several refinements were made in 2000, resulting in the modified Duke criteria [9]. These criteria incorporate clinical, laboratory, pathologic and echocardiographic criteria, and stratify patients into three main categories—definite IE, possible IE, and rejected—based upon the presence of major and minor criteria (Tables 16.2 and 16.3). "Definite" IE is defined by the presence of two major criteria, or one major and three minor, or five minor criteria. "Possible" IE is defined by one major and one minor criterion, or three minor criteria. "Rejected" indicates absence of evidence supporting the diagnosis of IE. For diagnosis, microbiologic confirmation (as demonstrated by positive blood cultures) is a principal

Table 16.3 Definition of endocarditis from modified Duke criteria

Definite infective endocarditis
Pathologic criteria
1. Microorganisms demonstrated by culture or histologic examination of a vegetation, a vegetation that has embolized, or an intracardiac abscess specimen; or
2. Pathologic lesions; vegetation or intracardiac abscess confirmed by histologic examination showing active endocarditis
Clinical criteria [a]
1. Two major criteria; or
2. One major criterion and three minor criteria; or
3. Five minor criteria
Possible infective endocarditis
1. One major criterion and one minor criterion; or
2. Three minor criteria
Rejected
1. Firm alternate diagnosis explaining evidence of infective endocarditis; or
2. Resolution of infective endocarditis syndrome with antibiotic therapy for ≤4 days; or
3. No pathologic evidence of infective endocarditis at surgery or autopsy, with antibiotic therapy for ≤4 days; or
4. Does not meet criteria for possible infective endocarditis, as above

From: Li JS et al [9]*; reproduced with permission, Oxford University Press*

(Modifications shown in boldface)

[a]See Table 16.2 for definitions of major and minor criteria

criterion. However, the Duke criteria clearly recognize and acknowledge the importance of echocardiography (with special mention of TEE) in the diagnosis of IE, as evidenced by the inclusion of echocardiographic findings as a major criterion for diagnosis. Indeed, echocardiography is now considered essential in the diagnostic workup and continuing evaluation of IE [10]. The utility of the Duke criteria have been validated by a number of studies in both the adult and pediatric populations [11–14]. They are now widely accepted guidelines for the evaluation of possible IE, both in adults as well as children [4, 15, 16].

The full diagnostic evaluation and management of IE encompasses a wide variety of aspects, including microbiology, antimicrobial therapy/duration, ongoing assessment, extracardiac complications, and indications and timing of surgical management [1, 17]. Therapy of IE is aimed at (a) eradication of the infecting microorganism; (b) treatment of cardiac complications; (c) prevention and/or treatment of extracardiac (particularly embolic) complications [1]. Antimicrobial therapy (selection/duration) is based upon the microbiology and susceptibility of the causative organism, and continues to evolve as new therapeutic agents are introduced. The role of surgery for IE also continues to evolve, and it is clear that this role has expanded; a recent European survey revealed that >50 % of adult patients with IE underwent surgery [18]. Controversy still exists as to the exact indications and timing for surgery; in most instances surgery is performed for left sided endocarditis, severe valvular involvement, and/or evidence of embolic phenomena [19]. Recently, there has also been published evidence that early surgery for severe left sided endocarditis in adults results in significantly better outcomes than conventional medical therapy [20]. Proposed indications and timing of surgery in adults are listed in Tables 16.4 and 16.5 [19]. In children, the indications for surgery are not as straightforward; surgery tends to be performed less frequently because 80–90 % of children with IE are expected to survive solely with conservative medical treatment [21, 22]. Nonetheless several published series of IE in children have reported an important percentage (between 16–67 %) of cases that required surgical intervention—in patients with and without CHD. In most published reports, the indications for cardiac surgery in pediatric IE patients tend to be similar to those of adults—valve dysfunction, congestive heart failure, septic embolization, and large vegetations. In addition, surgery is performed in CHD patients to repair the underlying cardiac defect (if still present), and also to remove or replace infected prosthetic material such as homografts and aortopulmonary shunts [7, 18, 21, 23–25].

Despite advances in medical and surgical management, IE remains a serious medical condition, with important risks of morbidity and mortality. A thorough and complete review of this multifaceted topic, including diagnosis, antimicrobial considerations, and medical/surgical therapy, would require its own separate chapter. For the purposes of this chapter, it is important to understand the integral role that echocardiography—and particularly TEE—plays in the many different aspects of the diagnosis and management of IE. This will be discussed below.

Echocardiographic Manifestations of IE

There are several ways in which IE can appear by echocardiography. The principal echocardiographic manifestations of IE include the following.

Vegetations

Vegetations are the most characteristic finding associated with endocarditis. They represent a mass of pathologic organisms nestled within a weave of platelets, red blood cells, and fibrin. Vegetations often develop in an area where the endothelium has been injured or disrupted by an abnormal high velocity jet or intravenous catheter; this usually occurs on a valvar surface, but can also be seen on a cardiac chamber wall when the endothelial surface has been injured. Vegetations also have the propensity to develop on foreign material such as a prosthetic valve or patch. The surface of the damaged endothelium or prosthetic material serves as a nidus for

Table 16.4 Indications for surgery in IE

Congestive heart failure[a]
Congestive heart failure caused by severe aortic or mitral regurgitation or, more rarely, by valve obstruction caused by vegetations
Severe acute aortic or mitral regurgitation with echocardiographic signs of elevated left ventricular end-diastolic pressure or significant pulmonary hypertension
Congestive heart failure as a result of prosthetic dehiscence or obstruction
Periannular extension
Most patients with abscess formation or fistulous tract formation
Systemic embolism[b]
Recurrent emboli despite appropriate antibiotic therapy
Large vegetations (>10 mm) after one or more clinical or silent embolic events after initiation of antibiotic therapy
Large vegetations and other predictors of a complicated course
Very large vegetations (>15 mm) without embolic complications, especially if valve-sparing surgery is likely (remains controversial)
Cerebrovascular complications[c]
Silent neurological complication or transient ischemic attack and other surgical indications
Ischemic stroke and other surgical indications, provided that cerebral hemorrhage has been excluded and neurological complications are not severe (e.g., coma)
Persistent sepsis
Fever or positive blood cultures persisting for >5–7 days despite an appropriate antibiotic regimen, assuming that vegetations or other lesions requiring surgery persist and that extracardiac sources of sepsis have been excluded
Relapsing IE, especially when caused by organisms other than sensitive streptococci or in patients with prosthetic valves
Difficult organisms
S aureus IE involving a prosthetic valve and most cases involving a left-sided native valve
IE caused by other aggressive organisms (Brucella, Staphylococcus lugdunensis)
IE caused by multiresistant organisms (e.g., methicillin-resistant staphylococcus aureus or vancomycin-resistant enterococci) and rare infections caused by Gram-negative bacteria
Pseudomonas aeruginosa or Fungal IE
Q fever IE and other relative indications for intervention
Prosthetic valve endocarditis
Virtually all cases of early prosthetic valve endocarditis
Virtually all cases of prosthetic valve endocarditis caused by staphylococcus aureus
Late prosthetic valve endocarditis with heart failure caused by prosthetic dehiscence or obstruction, or other indications for surgery

From: Prendergast and Tornos [19]; reprinted with permission from Walters Kluwer

[a]Surgery should be performed immediately, irrespective of antibiotic therapy, in patients with persistent pulmonary edema or cardiogenic shock. If congestive heart failure disappears with medical therapy and there are no other surgical indications, intervention can be postponed to allow a period of days or weeks of antibiotic treatment under careful clinical and echocardiographic observation. In patients with well tolerated severe valvular regurgitation or prosthetic dehiscence and no other reasons for surgery, conservative therapy under careful clinical and echocardiographic observation is recommended with consideration of deferred surgery after resolution of the infection, depending upon tolerance of the valve lesion

[b]In all cases, surgery for the prevention of embolism must be performed very early since embolic risk is highest during the first days of therapy

[c]Surgery is contraindicated for at least 1 month after intracranial hemorrhage unless neurosurgical or endovascular intervention can be performed to reduce bleeding risk

platelet/fibrin deposition, producing a thrombus (vegetation) at the site. This vegetation is at first sterile, but with bacteremia, circulating microorganisms can become adherent to the meshwork, resulting in an infected vegetation. Infection triggers further deposition of platelets and fibrin over the microorganisms; the organisms embedded within the vegetation are then shielded from host defense mechanisms, allowing them to proliferate rapidly and produce further growth of the vegetation [26]. Vegetations can have a number of detrimental effects: (a) they can grow and destroy adjacent tissue; (b) organisms can be released continuously into the bloodstream, leading to persistent bacteremia and hematogenous seeding of remote sites; (c) pieces of the vegetation can break off and embolize to other organs (brain, lung, kidney), sometimes producing serious and even devastating complications; (d) antibody response to the infecting organisms leads to subsequent tissue injury by immune complex deposition [1].

By echocardiography, vegetations are echogenic masses, generally irregular in shape and variable in size. They can localize anywhere on an affected valve or nonvalvar structure, though they tend to arise on a valve or endothelial surface "downstream" to a high velocity jet, e.g. adjacent to a ventricular septal defect or valvar regurgitant jet. They are usually freely mobile, oscillating with the cardiac cycle, and can move back and forth within the plane of a valve.

Table 16.5 Timing of Surgery

Emergency surgery (within 24 h)
Native (aortic or mitral) or prosthetic valve endocarditis and severe congestive heart failure or cardiogenic shock caused by:
Acute valvular regurgitation
Severe prosthetic dysfunction (dehiscence or obstruction)
Fistula into a cardiac chamber or the pericardial space
Urgent surgery (within days)
Native valve endocarditis with persisting congestive heart failure, signs of poor hemodynamic tolerance, or abscess
Prosthetic valve endocarditis with persisting congestive heart failure, signs of poor hemodynamic tolerance, or abscess
Prosthetic valve endocarditis caused by staphylococci or Gram-negative organisms
Large vegetation (>10 mm) with an embolic event
Large vegetation (>10 mm) with other predictors of a complicated course
Very large vegetation (>15 mm), especially if conservative surgery is available
Large abscess and/or periannular involvement with uncontrolled infection
Early elective surgery (during the in-hospital stay)
Severe aortic or mitral regurgitation with congestive heart failure and good response to medical therapy
Prosthetic valve endocarditis with valvular dehiscence or congestive heart failure and good response to medical therapy
Presence of abscess or periannular extension
Persisting infection when extracardiac focus has been excluded
Fungal or other infections resistant to medical cure

From Prendergast et al [19]; reprinted with permission from Walters Kluwer

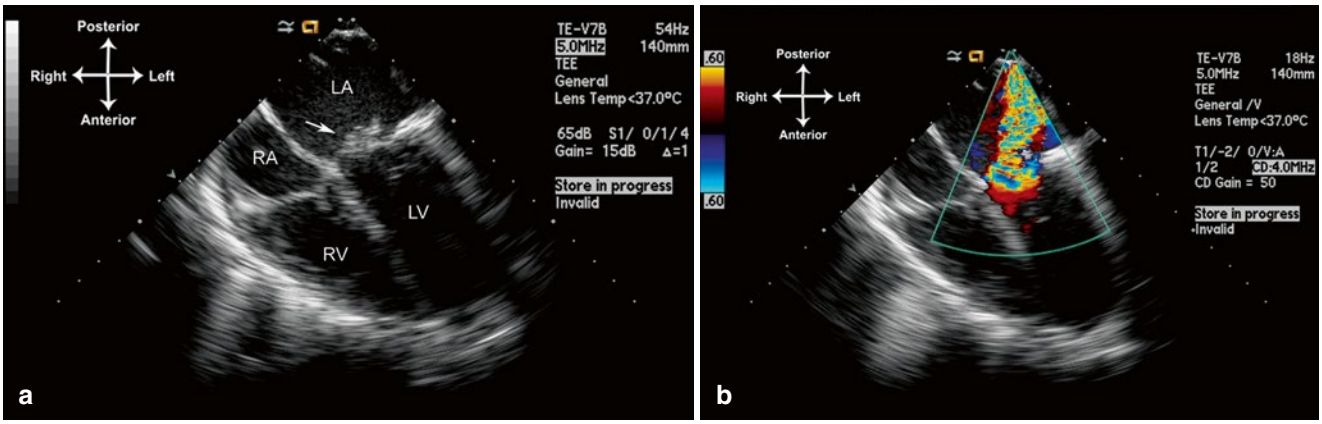

Fig. 16.1 Large vegetation (*arrow*) on the anterior leaflet of mitral valve (**a**), which resulted in chordal destruction and severe mitral regurgitation (**b**). Mid esophageal view four chamber (multiplane angle 0°). *LA* left atrium, *LV* left ventricle, *RA* right atrium, *RV* right ventricle

Intracardiac vegetations are generally very well seen by TEE (Fig. 16.1, Video 16.1).

Valvar Dysfunction

The echocardiographic manifestations of valvar dysfunction include ruptured chordae with prolapsing or flail leaflets, fenestrations in the valve cusps, and torn leaflets. All of these lead to disruption of valvar function and resultant valvar regurgitation, often to a significant degree. The amount of regurgitation, and the area of origin, can be well-seen using color flow Doppler. It is not uncommon to see vegetations in association with valvar disruption, as evidence of the destructive process from IE. Such patients not only appear toxic from their infection, but might also suffer symptoms of congestive heart failure if valvar incompetence is significant. Examples of valve disruption and accompanying vegetation are shown in Figs. 16.1 and 16.2, Videos 16.1 and 16.2.

Intracardiac Abscesses

Intracardiac abscess formation results from suppurative extension of the infective process. Purulent cavities form as the infection spreads into adjacent tissue. Most commonly, this occurs with native aortic valve IE, as infection extends into the weakest portion of the annulus—the membranous septum and atrioventricular node. When this occurs, heart block is a frequent sequela. Perivalvar abscess formation occurs in 10–40 % of all native IE; as noted, it is most common in native aortic valve IE, less common with native tricuspid or mitral IE [10]. Perivalvar abscesses are seen even

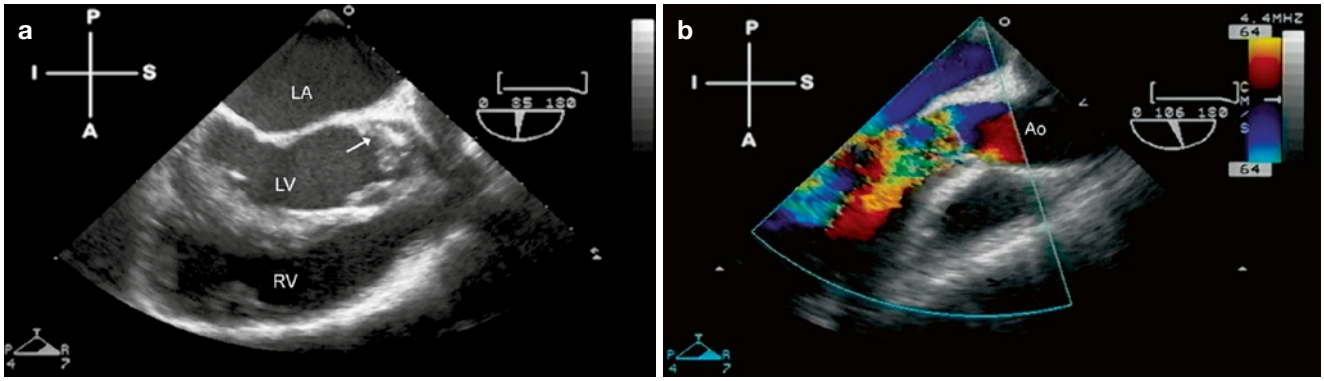

Fig. 16.2 Aortic valve endocarditis, seen from a mid esophageal aortic valve long axis view (multiplane angle 85°–106°). Figure **a** shows a prominent vegetation (*arrow*) on the left coronary cusp, which has caused significant cusp destruction and resulted in severe aortic valve regurgitation (**b**). *Ao* ascending aorta, *LA* left atrium, *LV* left ventricle, *RV* right ventricle

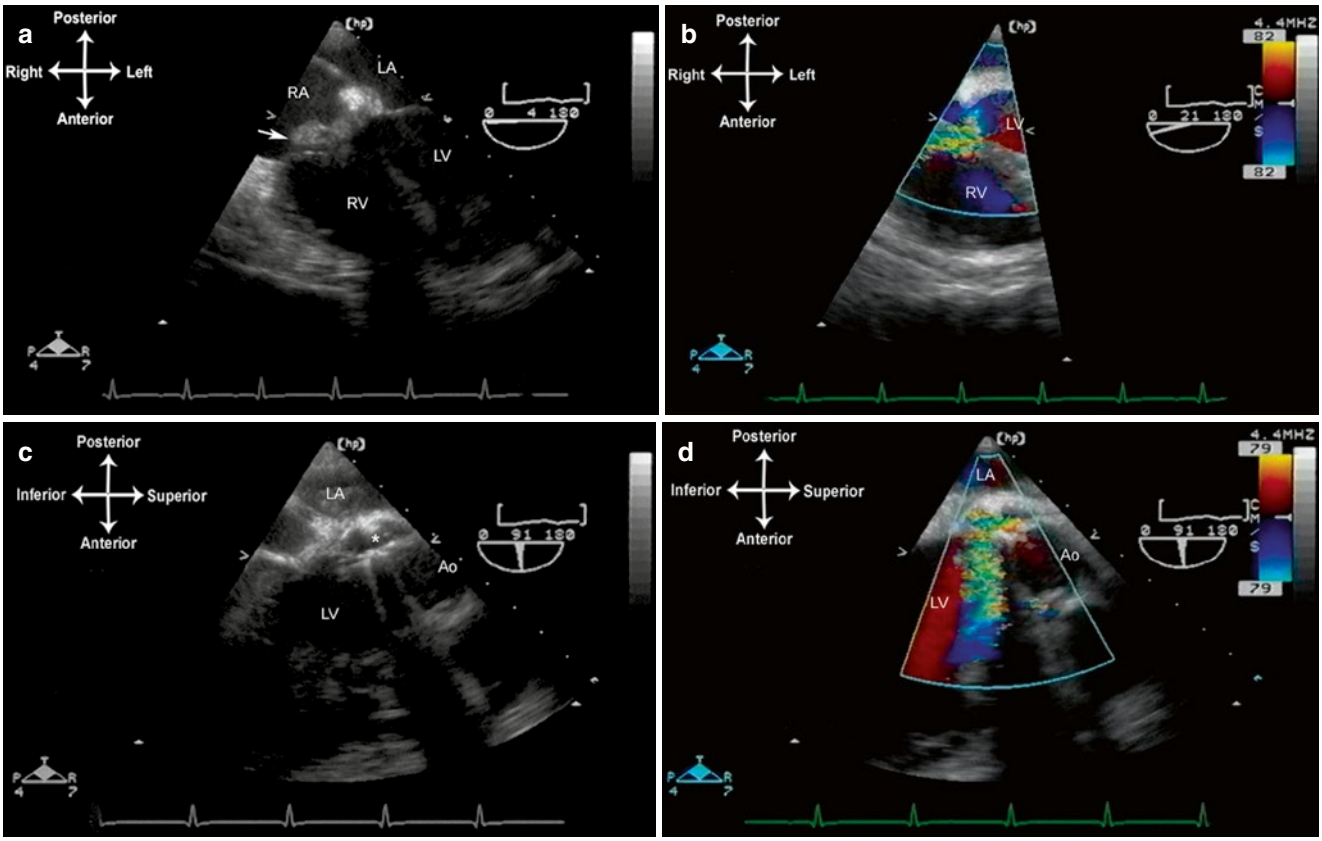

Fig. 16.3 Endocarditis in a patient with a prosthetic aortic valve (St. Jude bileaflet tilting disk valve). (**a**, **b**). The mid esophageal four chamber view demonstrates a perivalvar abscess that extends into the noncoronary cusp, causing a fistulous tract communicating with the right atrium. A large vegetation (*arrow*) has developed in this area and shunting is seen into the right atrium. (**c**, **d**). Mid esophageal aortic valve long axis view, angle about 90°. There is marked aortic regurgitation seen through an area of valve dehiscence (*). *Ao* aorta, *LA* left atrium, *LV* left ventricle, *RA* right atrium, *RV* right ventricle

more frequently with prosthetic valve IE, occurring in 56–100 % of patients [10, 27]. The characteristic echocardiographic appearance of abscess formation is as an echo-free space, representing purulent fluid, either within the wall surrounding the affected valve (e.g. the aortic root in aortic valve endocarditis), or extending into the adjacent tissue. In those patients with an abscess surrounding a prosthetic mitral valve, valve dehiscence is often seen. For the evaluation of abscesses, TEE has been shown to improve sensitivity dramatically compared to transthoracic echocardiography (TTE), and it is the preferred modality for diagnosis of perivalvar abscesses [28]. An example of an abscess that formed around a prosthetic aortic valve is shown in Fig. 16.3, Video 16.3.

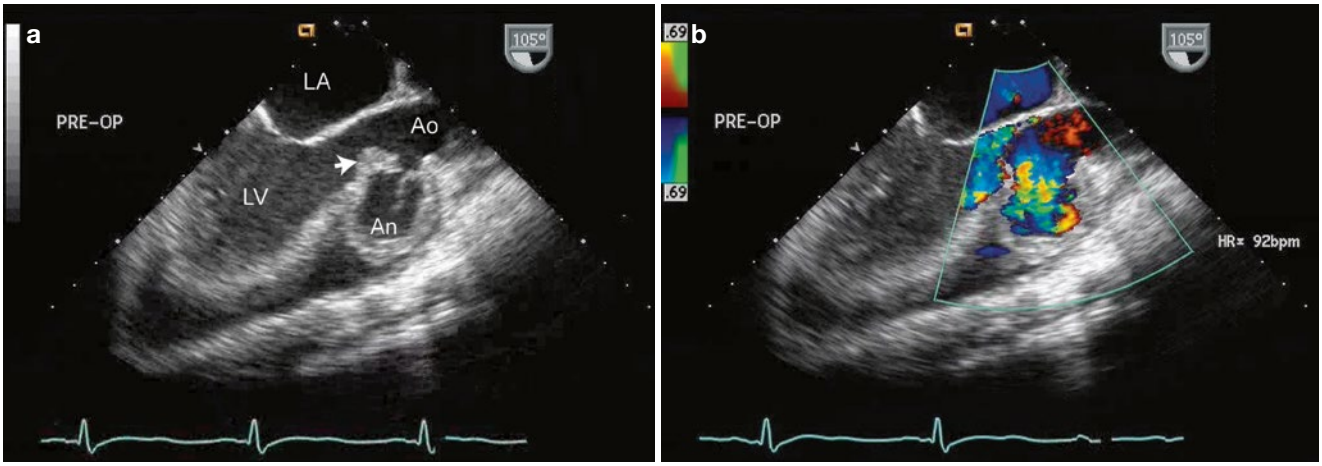

Fig. 16.4 Infected sinus of Valsalva aneurysm from aortic valve endocarditis, obtained from the mid esophageal aortic valve long axis view. Figure **a** shows a large vegetation of the aortic valve (*arrow*) and erosion of the right sinus of Valsalva, producing a large aneurysm (*An*). Figure **b** shows blood filling the aneurysm during diastole. *Ao* ascending aorta, *LA* left ventricle, *LV* left ventricle

Aneurysm Formation/Fistulous Tracts

If there is extension of the infection to the adjacent vessel wall, destruction of wall tissue can occur, leading to thinning and aneurysm formation. This can be seen especially with aortic valve IE, in which fistulous tracts can form between the sinus of Valsalva and an adjacent cardiac structure (i.e. an infected sinus of Valsalva aneurysm), or a fistulous tract can form into the pericardial space [29, 30]. In this setting, TEE will demonstrate the aneurysmal dilation of the vessel wall, and color flow Doppler will show systolic/diastolic (or continuous) flow between the aorta and the receiving chamber (Figs. 16.3 and 16.4, Videos 16.3 and 16.4). Infective endarteritis and pseudoaneurysm formation can also occur, particularly in areas of foreign material such as suture lines and biologic grafts [31, 32] (Fig. 16.5, Video 16.5).

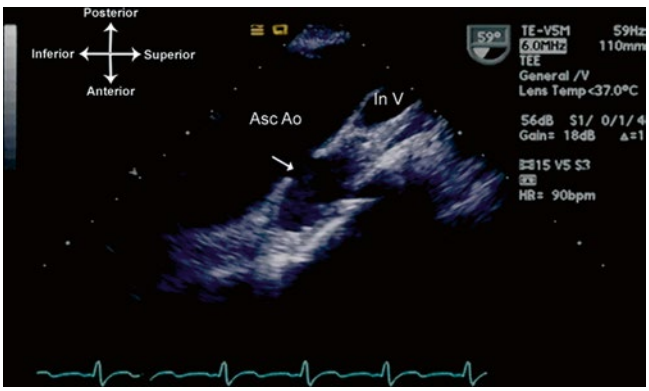

Fig. 16.5 Infected pseudoaneurysm off ascending aorta. This TEE was performed to evaluate the aortic valve in a patient with a previous aortic valve surgery and persistent fungemia. A large pseudoaneurysm (*arrow*) was discovered using an upper esophageal view, multiplane angle 60°. At surgery, the pseudoaneurysm was found to be infected and filled with fungus. Note that the superior portion of aorta and innominate vein can be seen well in this patient by TEE. *Asc Ao* ascending aorta, *In V* innominate vein

Congestive Heart Failure/Pericardial Effusion

Congestive heart failure (CHF) is a known complication of IE, and one associated with a poor prognosis [33–35]. It can occur as a result of several different complicating processes associated with IE: native valve destruction/perforation/chordal rupture, prosthetic valve dehiscence, abscess formation causing heart block, sudden intracardiac shunts due to fistulous tracts, and septic emboli to the coronaries causing myocardial ischemia/infarction [10, 19]. In addition, myocardial dysfunction can be seen with IE, either from myocardial toxicity due to the IE process (e.g. large abscess), ventricular decompensation from valvar regurgitation, or the overall septic process causing generalized depression of myocardial function (particularly with a virulent organism such as *Staphylococcus aureus*). In native valve IE, acute CHF is more frequently seen with left sided infections—aortic (29 %) and mitral (20 %)—than with tricuspid infections (8 %) [10]. A pericardial effusion can also be seen in patients with IE; it can be infectious, resulting from hematogenous seeding of the pericardium or as a direct extension from intracardiac IE (e.g. perforation of a perivalvar abscess). Rarely, it can occur as a reactive/serous effusion [36].

Use of TEE for Evaluation of Infective Endocarditis

As noted above, echocardiography is considered essential in the diagnosis and management of IE. The major question is whether to perform TTE or use TEE to evaluate for vegetations. In adults, a number of studies have confirmed the superior diagnostic sensitivity of TEE over TTE for IE [37–40]. This is particularly true in those patients with

intracardiac abscesses and prosthetic valve endocarditis, in whom TEE appears clearly superior for diagnosis [28, 41]. In children, the advantages of TEE over TTE are less apparent, particularly with the infant and younger child, in whom TTE generally provides excellent imaging. For younger pediatric patients, TTE is usually adequate for the diagnostic evaluation of IE [42]. In most pediatric patients, particularly the younger age groups, the evidence suggests that TEE can be reserved for those patients in whom imaging quality is felt to be suboptimal. A recent study in pediatric patients ages 10 days to 17.5 years (over half of whom had CHD) showed that TTE, when used in conjunction with the Duke criteria, was useful for the diagnosis of IE; the authors recommended TEE only for an "inadequate" TTE study or when there was an organism with a high association of aortic root abscess [43].

The evaluation of IE by TEE can occur in several settings. It can be performed in the ICU or ambulatory setting, serving as either diagnostic evaluation for suspected IE or as a monitoring procedure for a patient receiving treatment for known IE. It also plays a vital role in the operating room. Preoperatively, TEE is used to assess not only the vegetation or abscess, but also valvar function and the surrounding cardiac structures. When applicable, prosthetic valve dehiscence and pseudoaneurysm formation can also be evaluated. Postoperatively, TEE is used to assess the results of operative repair or valve replacement, and to guide perioperative hemodynamic management [19, 36].

If TEE is performed to evaluate for IE, a complete study should be performed using all major TEE views/windows, as outlined in Chap. 4. Assessment should focus on a number of details. If a vegetation is present, its appearance and motion should be evaluated in multiple planes, and linear measurements can be obtained. The risk of embolic events appears to be greatest with vegetations >10 mm on the anterior leaflet of mitral valve [44]. Valve leaflet anatomy and motion should also be evaluated both by imaging and color flow Doppler, with attention paid to any valvar perforation or chordal disruption. In the case of aortic valve endocarditis, a careful evaluation should also be made for possible abscess or aneurysm formation. If a prosthetic valve is in place, a thorough assessment should be performed for vegetations, valve leaflet motion, and possible perivalvar abscess/dehiscence. Color flow Doppler is useful to determine valve competency and flow profile. A complete evaluation should be performed of other cardiac structures to rule out structural defects and/or other potential sites of IE, including the aorta and pulmonary artery (when the pulmonary artery can be visualized by TEE). Rarely, cases of endarteritis can also be found by TEE (Fig. 16.5, Video 16.5). Finally, myocardial function should also be assessed.

Three caveats are important to consider. First, even with TEE, not all vegetations will be visible, particularly if the vegetations are smaller than the resolution limits of the TEE probe and/or TEE imaging is suboptimal. This is an important consideration in patients with operated and unoperated CHD, who can have vegetations located in areas not readily visible by TEE (e.g. a Blalock-Taussig shunt). Studies have shown that—irrespective of whether TTE or TEE is used—patients with CHD and IE are less likely to have visible vegetations [5]. Thus, the echocardiographic data should be considered in the context of the entire clinical picture, as noted with the Duke criteria listed above. In some cases, if IE is still suspected, a TTE or TEE can be performed 7–10 days later to determine if a vegetation or abscess has appeared [10]. The second important caveat is that not all echogenic masses represent vegetations. Sterile thrombi, tumors, irregular valve excrescences, and foreign material (such as suture material) can sometimes resemble vegetations. Again, the echocardiogram should be reviewed in conjunction with the entire clinical picture. If previous echocardiograms are available (either transthoracic or transesophageal), these can be very useful to make direct comparisons to determine whether an abnormal finding is new or longstanding. New findings are much more suspicious for IE. The last important caveat is that not all vegetations are infectious. A number of medical conditions can produce sterile vegetations adherent to valvar surfaces. Examples of these include systemic lupus erythematosus (Libman-Sachs endocarditis), and nonbacterial thrombotic endocarditis (NBTE, also known as marantic endocarditis). The latter can occur as complication of malignancy, uremia, burns, hypercoagulable states, or autoimmune diseases, and it has been found in approximately 1.2 % of all autopsy patients, although the reported incidence is between 0.3–9.3 % [1, 45]. In fact, Libman-Sachs endocarditis is felt to be a form of NBTE [46]. These vegetations are usually seen on the valve closure contact line of the atrial surface of the atrioventricular (AV) valves and ventricular surface of the semilunar valves. In many cases, the vegetations are benign and clinically inapparent. However, systemic embolization has been described in up to 30–50 % of patients [45–47], with a tendency towards embolization to the brain, kidney, spleen, mesenteric bed, or extremities [46, 48].

Cardiac Masses

Aside from infective endocarditis, the most common pathologic cardiac masses are thrombus or tumors. The role of TEE in the diagnostic assessment of cardiac masses is generally complementary to TTE, particularly in pediatric patients. In most cases, TTE is more than adequate to evaluate the location and extent of a cardiac mass. However in older patients, and in those with poor echocardiographic windows, TEE might be called upon to assist in evaluation. For instance, TEE has become well established in adults as a

requisite tool for evaluation of the etiology of ischemic strokes; approximately 15–20 % are caused by cardiogenic emboli (thrombi, tumors, vegetations, etc.) [49].

Cardiac Thrombi

Thrombi can vary considerably in their echocardiographic appearance and location. They are generally echogenic, relatively homogeneous in density, and irregular in shape. In some instances there can be calcification within the thrombus. They are generally attached to some structure in the heart, whether it is an endocardial surface, AV valve, or some type of foreign material. The attachment point is usually broad-based, but it can also be thin and pedunculated in appearance. In most clinical settings, thrombi are associated with an indwelling catheter, although in certain pathologic situations—e.g. where there is stasis of blood—they can arise spontaneously. An important example of this is dilated cardiomyopathy, in which reduced cardiac motion leads to stasis of blood flow and a propensity for thrombus formation, particularly near the apex of the left ventricle (Fig. 16.6, Video 16.6). In those situations in which a catheter is present, usually the superior vena cava (SVC) or right atrium, TEE can be used to evaluate the attachment point, size, and extent of the thrombus. Mid to upper esophageal views, with the probe rotated rightward and multiplane angle 80–95° (mid esophageal bicaval view), permit a sagittal visualization of the length of the SVC as it returns to the right atrium (Fig. 16.7, Video 16.7). If an indwelling catheter is present, it can be visualized and evaluated for a possible attached thrombus. It is important not to misinterpret normal structures or variants, such as the crista terminalis (the muscular ridge in the interior of the right atrium separating right atrial appendage from the remainder of the atrium), as an intracardiac thrombus. Color flow Doppler can evaluate the flow returning through the SVC to the right atrium. If there is obstruction to SVC return, a mean gradient can sometimes be obtained using the deep transgastric views (long axis and sagittal), rightward turning of the probe, and anteflexion to achieve posterior angulation (see Chap. 4). These maneuvers enable visualization of SVC flow as it enters the right atrium, and also provide an excellent angle of insonation for spectral Doppler interrogation.

Thrombi sometimes develop in the left (and less frequently, the right) atrial appendage in patients, particularly adults with severe mitral stenosis and/or atrial fibrillation [50, 51]. In adult studies, the incidence of left atrial thrombus in patients with atrial fibrillation ranges between 10–15 %, and right atrial thrombus 0.4–7.5 % [52]. These thrombi are often challenging to visualize by TTE [53]. It can also be difficult to distinguish these thrombi from pectinate muscles. In this setting, TEE proves invaluable because of the close proximity of the esophagus to both atria, providing excellent visualization of all atrial structures, including the atrial

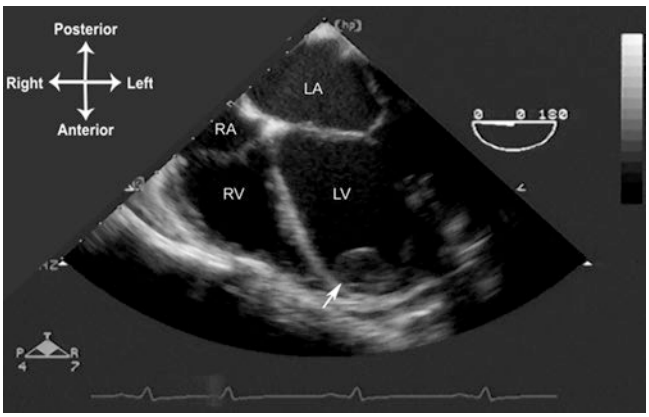

Fig. 16.6 Thrombus (*arrow*) in the left ventricular apex of a patient with Duchenne muscular dystrophy and dilated cardiomyopathy. Mid esophageal four chamber view, multiplane angle 0°. *LA* left atrium, *LV* left ventricle, *RA* right atrium, *RV* right ventricle

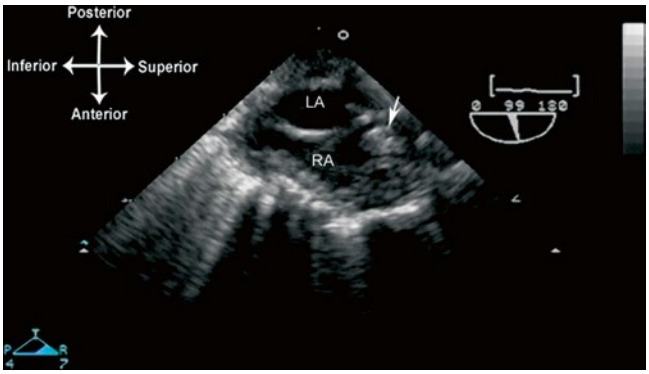

Fig. 16.7 Thrombus (*arrow*) in the superior vena cava, probably associated with a catheter. Seen from mid esophageal bicaval view, (multiplane angle 99°). *LA* left atrium, *RA* right atrium

appendages [54, 55]. The left atrial appendage can be well visualized by TEE using the mid esophageal views and leftward rotation, with slight anteflexion to bring the appendage into view (Fig. 16.8, Video 16.8). Rotating the multiplane angle between 0° and 90° affords different views of the structure. The right atrial appendage is best seen from the mid esophageal bicaval view, multiplane angle 85–90°; it is seen anterior to the SVC/right atrial junction. The multiplane angle can also be rotated to 0° to visualize the right atrial appendage from a different plane. Again, it is important to inspect carefully both the right and left atrial appendages, and to distinguish pectinate muscles and multiple appendage lobations [56] from actual thrombus [54, 57].

There are certain normal anatomic structures that can resemble a thrombus, and must therefore be inspected carefully by TEE. As previously noted, the crista terminalis can occasionally be mistaken as a thrombus. A Chiari network can sometimes be confused for a thin thrombus or vegetation. This structure, an embryologic remnant of the right valve of the sinus venosus, is usually very mobile and can exhibit considerable

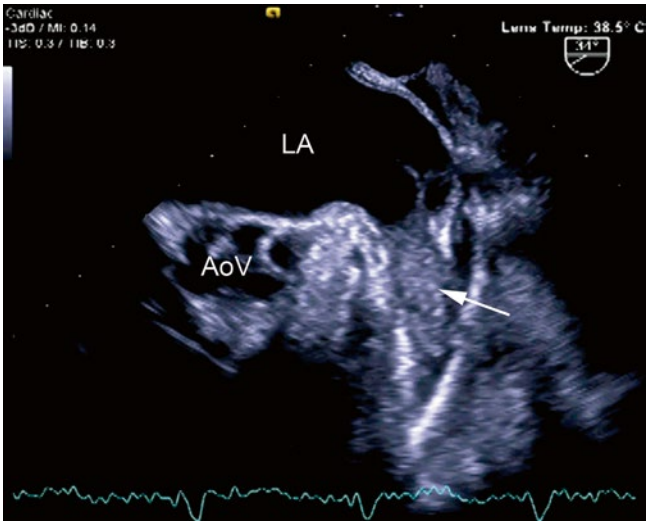

Fig. 16.8 Thrombus in the left atrial appendage (*arrow*), as viewed from a modified mid esophageal aortic valve short axis view with leftward rotation. There are mobile filamentous strands arising from the thrombus. *AoV* aortic valve, *LA* left atrium (Photograph courtesy of Siemens Medical Systems USA, Inc. © 2012–13 Siemens Medical Solutions USA, Inc. All Rights Reserved)

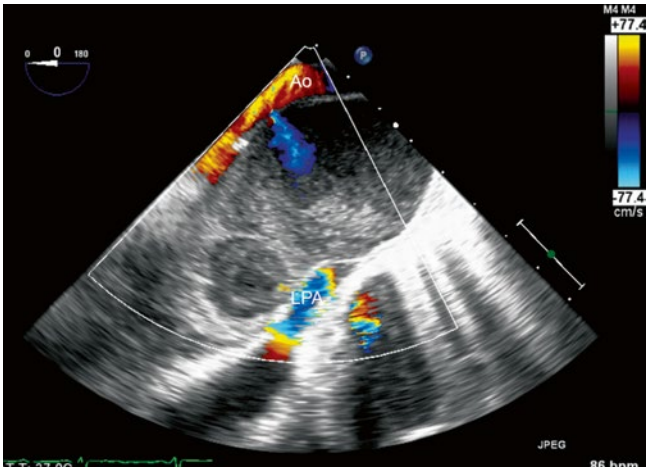

Fig. 16.9 Example of spontaneous echo contrast in a patient after repair of D-transposition of the great arteries, with a pseudoaneurysm arising from a previous cannulation site in the aorta. Image obtained from the upper esophageal aortic arch long axis view. Note the visible swirling of flow due to red cell aggregation. The left pulmonary artery (*LPA*) is compressed by the pseudoaneurysm. *Ao* ascending aorta

anatomic variation [58]. It is attached to the Eustachian and Thebesian valves; it is thin and redundant and often displays a porous, fenestrated or filamentous appearance. A related structure, a prominent Eustachian valve, can be very prominent and extend into the right atrium. It can also be very mobile, and in some cases has the appearance of long vegetation or thrombus. Both a Chiari network and Eustachian valve are well seen using the mid esophageal bicaval view, with multiplane angle approximately 80–90°. In the left atrium, a prominent ridge between left upper pulmonary vein and left atrial appendage (sometimes informally called the "coumadin ridge") can, on occasion, be mistaken for a thrombus. Another important artifact that may resemble an intracardiac thrombus is the presence of spontaneous echo contrast, or "smoke", in an atrial chamber [50, 59, 60]. This represents red cell aggregation from sluggish blood flow, such as that seen in a low-flow Fontan circuit (Chap. 10). When dense and echogenic, it can produce the appearance of thrombus. However, the swirling and circular movements differentiate this type of finding from a thrombus (Fig. 16.9, Video 16.9).

Cardiac Tumors

Cardiac tumors are divided into two categories: primary and secondary/metastatic. Primary cardiac tumors originate in the heart, and most of these are benign [61–64]. However despite their "benign" histopathology, some primary tumors can still cause significant clinical sequelae due to arrhythmias, mass effect (obstruction), or embolization. Rarely, primary cardiac tumors are malignant and, if so, they are usually sarcomas and are almost always associated with a poor outcome [62]. The other class of cardiac tumors comprises the secondary/metastatic tumors that are, by definition, malignant. Secondary cardiac tumors occur mostly as distant metastases, but they can also invade the heart by direct extension, for example via the inferior vena cava (IVC). Secondary malignant cardiac tumors are seen much more frequently than primary cardiac tumors, both in adults and children. Indeed, in the adult literature metastatic tumors outnumber primary cardiac tumors by a 20–30 to 1 ratio, and in children, by a 3–4 to 1 ratio [61, 62]. In adults, the most common primary sites for metastasis to the heart include lung, breast, lymphoma/leukemia, esophageal, uterine and melanoma. Most of these metastases are to the pericardium, and 90 % are clinically silent [63]. In children, the most common tumors with metastasis to the heart are non-Hodgkin's lymphoma, neuroblastoma, Wilms tumor, and soft tissue/bone sarcomas [61]. Direct extension of a tumor can occur from the IVC to the right atrium in patients with Wilms tumor [65], renal myosarcoma, or adrenal and hepatocellular carcinoma (Fig. 16.10, Video 16.10). As with adults, overt clinical signs and symptoms of secondary tumors are uncommon [61].

The echocardiographic presentation of cardiac tumors is highly variable, depending upon the type of tumor and the site of involvement. Cardiac tumors can involve only endocardium, only myocardium, only pericardium, or various combinations thereof [62]. There can be one or multiple foci, again depending on tumor type. An extensive discussion of cardiac tumors is beyond the scope of this chapter, and there are other excellent references available on the subject [62, 63, 66]. The remainder of this section will discuss a few of the more common primary cardiac tumors and

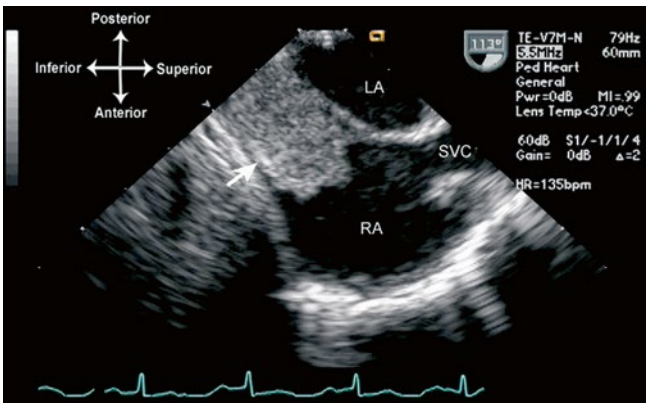

Fig. 16.10 Wilms tumor (*arrow*) invading the right atrium by direct extension from the inferior vena cava, as seen from the mid esophageal bicaval view, multiplane angle 113°. *LA* left atrium, *RA* right atrium, *SVC* superior vena cava

provide examples of their evaluation by TEE. The method of TEE evaluation for these particular tumors can be applied to the evaluation of cardiac tumors of any etiology.

Rhabdomyoma

Rhabdomyomas are the most commonly encountered primary cardiac tumors in the pediatric age group, comprising approximately 60–80 % [67, 68]. Typically, multiple tumors are located within the free wall of the right and left ventricle, as well as the interventricular septum. They can also be present in the right atrium. There is a strong association (at least 50 %) with tuberous sclerosis. These tumors are histologically benign but nevertheless patients can be clinically symptomatic in a number of different ways. Depending upon location, atrial or ventricular arrhythmias can occur. Tumors of sufficient size adjacent to an area of inflow or outflow can cause significant obstruction, which occasionally necessitates surgical resection. However with time, spontaneous regression of these tumors usually occurs, so surgery is not indicated in most patients unless the tumors cause significant mass effect.

Given the generally benign nature of cardiac rhabdomyomas, and the young age that these tumors are first diagnosed, it is very rare that a TEE is necessary for evaluation; TTE generally suffices. The major indication for TEE is in patients undergoing surgery for relief of inflow or outflow tract obstruction. Rhabdomyomas are characteristically homogenous, echogenic, and well circumscribed; they are easily distinguished from the surrounding myocardium. The mid esophageal four chamber (ME 4 Ch) view (multiplane angle 0°) is the best view from which to begin evaluation of the tumors, both ventricular and (if present) atrial. Once located, they can be visualized more closely with variations in multiplane angle, along with anteflexion and retroflexion to bring the tumor(s) into view. If a large tumor is causing possible obstruction to AV inflow, color flow and spectral Doppler should be used to evaluate for disturbed flow patterns around the tumor, and to determine a mean gradient across the area. If the tumor is causing possible outflow tract obstruction, mid esophageal views such as the ME 4 Ch, mid esophageal long axis (ME LAX), and mid esophageal right ventricular inflow-outflow (ME RV In-Out) with multiplane angles varying between 0° to 110° are best to evaluate the anatomic extent of the tumor and any turbulence as seen by color flow Doppler (Fig. 16.11, Video 16.11). Deep transgastric long axis (DTG LAX) and deep transgastric sagittal (DTG Sagittal) views with probe anteflexion/retroflexion provide the best angle of spectral Doppler interrogation of the ventricular outflow tracts. The transgastric views also provide other perspectives from which to visualize both right and left sided tumors. These views include the transgastric basal short axis (TG Basal SAX), mid short axis (TG Mid SAX), two chamber (TG 2 Ch), long axis (TG LAX), and right ventricular inflow (TG RV In).

Fibroma

Fibromas are the second most common cardiac tumor encountered in the pediatric age group (10–30 %) [69]. They are generally solitary and intramural, located within the ventricular septum or left ventricular free wall [62]. When large, they can impinge significantly upon the adjacent cardiac chamber (usually the left ventricle), causing symptomatology such as congestive heart failure and cyanosis. Rarely, they can be multiple and involve other parts of the heart including the ventricular conduction system, right ventricle and right ventricular free wall. They frequently cause ventricular arrhythmias [70]. Because these tumors do not regress spontaneously and sometimes can grow significantly, surgical resection is recommended.

The TEE evaluation of fibromas generally occurs in the operating room setting, and is similar to that involved with the evaluation of other cardiac tumors. The tumors are best seen using the mid esophageal views, with a combination of multiplane angles between 0° and 100°. Color flow and spectral Doppler should be employed to evaluate for potential compromise of ventricular inflow or outflow due to the tumor. The echocardiographic appearance of a fibroma is that of a single, bright, echo-dense intramural mass with calcifications and cystic areas within the tumor (Fig. 16.12, Video 16.12).

Myxoma

Myxomas represent the most common primary cardiac tumor in adults [62, 71]. On occasion, they can also be seen in children. They are most commonly located in the left atrial cavity (75–90 %), but can also be found in the right atrium [72], as well as the ventricles [62, 73]. Rarely, they can be present in more than one cavity [74]. Clinical

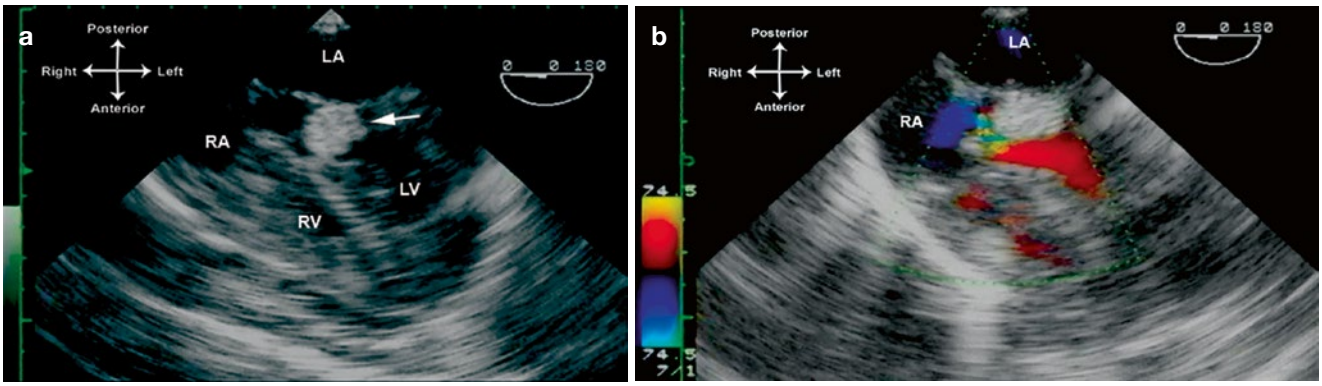

Fig. 16.11 Multiple rhabdomyomas in a patient with tuberous sclerosis, including one that caused near complete obstruction of the left ventricular outflow tract. Figure **a** is obtained from a mid esophageal four chamber view, multiplane angle 0°, showing a large tumor in the outflow tract (*arrow*). Turbulent color flow Doppler is seen in (**b**). This tumor was resected surgically. *LA* left atrium, *LV* left ventricle, *RA* right atrium, *RV* right ventricle

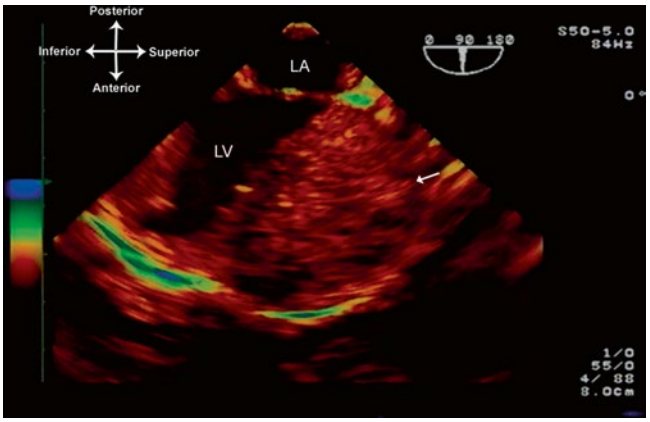

Fig. 16.12 Fibroma attached to the left ventricular free wall, visualized from mid esophageal long axis view, multiplane angle 90°. The fibroma (*arrow*) is very large, circumscribed, and has a heterogeneous appearance, studded with echolucent areas most likely representing cystic degeneration or necrosis. *LA* left atrium, *LV* left ventricle

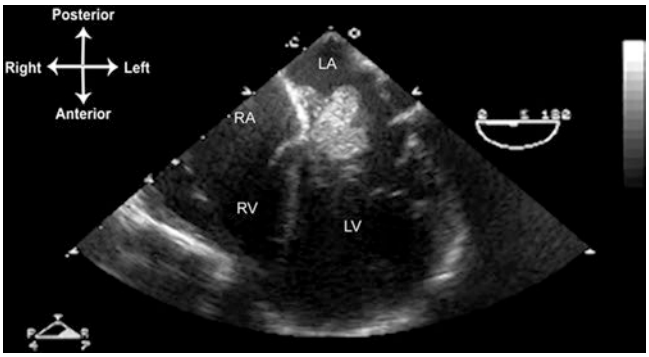

Fig. 16.13 Left atrial myxoma, seen from mid esophageal four chamber view, multiplane angle 0°. A large, lobulated myxoma is attached to the interatrial septum just posterior to the aortic root. *LA* left atrium, *LV* left ventricle, *RA* right atrium, *RV* right ventricle

manifestations of a left atrial myxoma are quite variable and can include embolic phenomena and/or obstruction to blood flow causing breathlessness, syncope, and congestive heart failure. Other constitutional symptoms such as fever, malaise, weight loss, and myalgias/arthralgias can also be present. Familial occurrence is reported in approximately 7–10 % of all myxomas, generally in younger patients. These are associated with multiple endocrine syndromes including LAMB (lentigines, atrial myxoma, mucocutaneous myxoma, and blue nevi) and NAME (nevi, atrial myxoma, neurofibromata, and ephelides).

Myxomas are gelatinous in consistency and they can be pedunculated. By echocardiography, they have a globular, lobulated, or fimbriated appearance, and a pedicle can be present. There may be small lucencies and calcifications in the tumor, resulting in an inhomogeneous appearance. Left atrial myxomas characteristically have attachments to the atrial septum, but they can also attach to other portions of the left atrium or to the mitral valve. If large enough, the myxoma can cause obstruction to mitral inflow. Given the numerous potential complications, including embolus, the treatment for atrial myxomas is surgery, and TEE plays an important role in the pre and postoperative assessment [75]. The attachment point, the extent of the tumor, the number of tumors, and relationship to surrounding structures, should all be evaluated carefully prior to surgical resection. Following surgery, it is important for TEE assessment to include evaluation of the left atrium and interatrial septum, in order to determine completeness of tumor resection as well as the integrity of the mitral valve. Atrial myxomas are best visualized by TEE with the mid esophageal views, using several multiplane angles to determine the location and extent of the tumor (Fig. 16.13, Video 16.13). Color flow and spectral Doppler should be used to evaluate any obstruction to mitral valve inflow, and/or mitral regurgitation resulting from damage to the mitral valve leaflets or valve interference by the tumor.

Other Cardiac Tumors

Hemangiomas and teratomas are two other primary tumors that are occasionally encountered in the pediatric population. Hemangiomas can be located anywhere within the heart, but have a predilection for the right atrium and ventricular septum [76]. By echocardiography, there are numerous echolucent spaces, and color flow Doppler often demonstrates multiple vascular channels (Fig. 16.14, Video 16.14). Teratomas are usually detected in the fetus and neonate. They most commonly occur in the pericardial space, but can also arise within the heart, attached to the atrial or ventricular wall. When in the pericardial space, they are often attached to the aortic root or pulmonary trunk, and they can grow to a large size. There may be an associated pericardial effusion. If sufficiently large, either the tumor or the effusion (or both) can compress the heart, leading to tamponade physiology. When intracardiac in location, these can cause clinical signs and symptoms similar to other intracardiac tumors. By echocardiography, the tumors appear heterogeneous and encapsulated [67].

Role of TEE in the Evaluation of Cardiac Tumors

Most cardiac tumors are well seen by TTE, particularly in younger patients, and therefore TTE serves as the principal modality for their evaluation and follow-up. Cardiac magnetic resonance imaging has become increasingly utilized for diagnostic evaluation of cardiac tumors [77–79]. The role of TEE is primarily for two settings: (a) for those patients in whom TTE imaging is poor or incomplete, and (b) for intraoperative assessment. Specifics of optimal TEE probe location and multiplane angles, along with methods of evaluation, will depend upon the type and location of the tumor (as detailed above). In adults, TEE has been reported to provide more precise depiction of tumor attachment sites and extent of myocardial/pericardial involvement [80, 81]. Intraoperatively, the preoperative TEE study is used to confirm the nature and extent of tumor involvement [82, 83]. The postoperative TEE study evaluates the results of cardiac surgery—focusing on completeness of tumor resection residual obstruction (if previously present), whether any adjacent cardiac structures (e.g. cardiac valves) might have been affected by the resection, and assessment of ventricular function [84, 85].

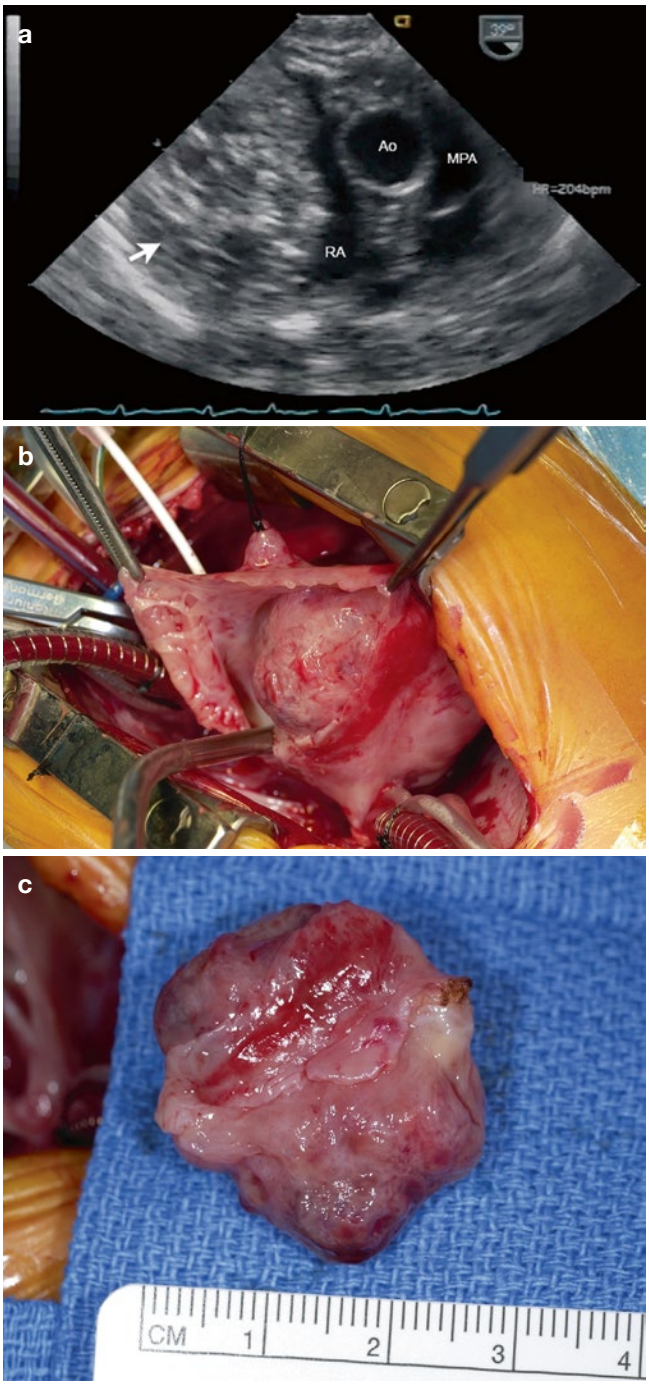

Fig. 16.14 Right atrial hemangioma as seen from a modified mid esophageal right ventricular inflow-outflow view. (**a**) Note the markedly heterogeneous nature of the large mass in the right atrium (*arrow*). The patient underwent surgery and the tumor was removed (**b** and **c**). *Ao* ascending aorta, *MPA* main pulmonary artery, *RA* right atrium

Evaluation of Prosthetic Valves

Prosthetic valves are integral to the medical and surgical management of pediatric and adult patients with CHD. These valves fall into two major categories—mechanical and biologic—based upon valve composition (Table 16.6).

Mechanical heart valves contain nonbiologic materials (polymers, metal, carbon) in all parts of the prosthesis: the valve ring, sewing cuff, and orifice occluder. A number of mechanical valves have been developed over the past 50 years, essentially of three major types. The first type to be developed was the caged ball valve, consisting of a silastic ball with a circular sewing ring and a cage formed by three metal arches. The most notable of these was the

Starr-Edwards valve (Fig. 16.15c), though similar valves have been produced including the Smeloff-Cutter valve. While these valves are no longer implanted, thousands of patients who received these valves are still alive, and continue to be followed regularly. The second type of mechanical valve is the monoleaflet valve, in which a single disk is secured by lateral or central metal struts, and surrounded by a sewing ring. The disk, generally made of extremely hard carbon (pyrolytic carbon), opens by tilting at an angle (about 60°–80°), resulting in two orifices of different sizes. Typical examples of this include the Bjork-Shiley (discontinued), and the Medtronic-Hall valve (Fig. 16.15b). The third major type of mechanical valve is the bileaflet tilting disk valve, made of two semicircular pyrolytic carbon disks attached by hinges to a rigid valve sewing ring. In the open position the valve leaflets tilt to an opening angle of 75°–90°, resulting in three orifices: a small slit-like orifice centrally between the two leaflets, and two semicircular orifices laterally. Of the three types of mechanical valves, the bileaflet tilting disk valve provides the most natural blood flow, greater effective orifice area for a given valve size, and it is also the least thrombogenic. Currently, they are the most commonly implanted mechanical valves, notably the St. Jude Medical (Fig. 16.15a) and Carbomedics bileaflet tilting disk valves. The latter two valves are available in a variety of sizes (from 16–33 mm) suitable for both pediatric and adult patients. The mechanical valves have a proven record of durability, however they require ongoing anticoagulation therapy, and there

Table 16.6 Typical biologic and mechanical valves

Valve name/type	Manufacturer	Valve type/origin
Biologic—Human		
Autograft		Pulmonary autograft
Allograft (Homograft)	Cryolife	Harvested cadaveric aortic, pulmonary homograft
Monocusp, bicuspid		Surgically handsewn valve using autologous pericardium
Biologic—Heterograft		
Stented		
Hancock II	Medtronic	Porcine
Mosaic	Medtronic	Porcine
Carpentier-Edwards	Edwards-Lifesciences	Porcine
Epic	St Jude	Porcine
Biocor	St Jude	Porcine
Trifecta	St Jude	Bovine pericardial
Carpentier-Edwards Perimount Magna	Edwards Lifesciences	Bovine pericardial
Mitroflow	Sorin Biomedica	Bovine pericardial
Soprano	Sorin Biomedica	Bovine pericardial
Stentless		
Freestyle	Medtronic	Porcine
Toronto SPV	St Jude	Porcine
Prima Plus	Edwards Lifesciences	Porcine
Pericarbon Freedom	Sorin Biomedica	Bovine pericardial
3 F Therapeutics Stentless Equine	3 F Therapeutics	Equine pericardial
Mechanical		
Starr-Edwards	Edwards Lifesciences	Ball-in-cage
Bjork-Shiley	Pfizer	Single leaflet tilting disk
Medtronic-Hall	Medtronic	Single leaflet tilting disk
St. Jude Medical	St Jude	Bileaflet tilting disk
CarboMedics	Sorin-CarboMedics	Bileaflet tilting disk
ATS Medical	ATS Medical	Bileaflet tilting disk
On-X	On-X Life Technologies	Bileaflet tilting disk
Percutaneous—Biologic		
Melody	Medtronic	Bovine jugular valve mounted on platinum-iridium stent
SAPIEN	Edwards Lifesciences	Bovine pericardium leaflets mounted on stainless steel or cobalt chromium alloy (SAPIEN XT)
CoreValve	Medtronic	Porcine pericardium leaflets mounted on self-expanding nitinol frame
Other		
SynerGraft	Cryolife	Tissue engineered decellularized allograft heart valve
Contegra	Medtronic	Valved conduit of bovine jugular vein

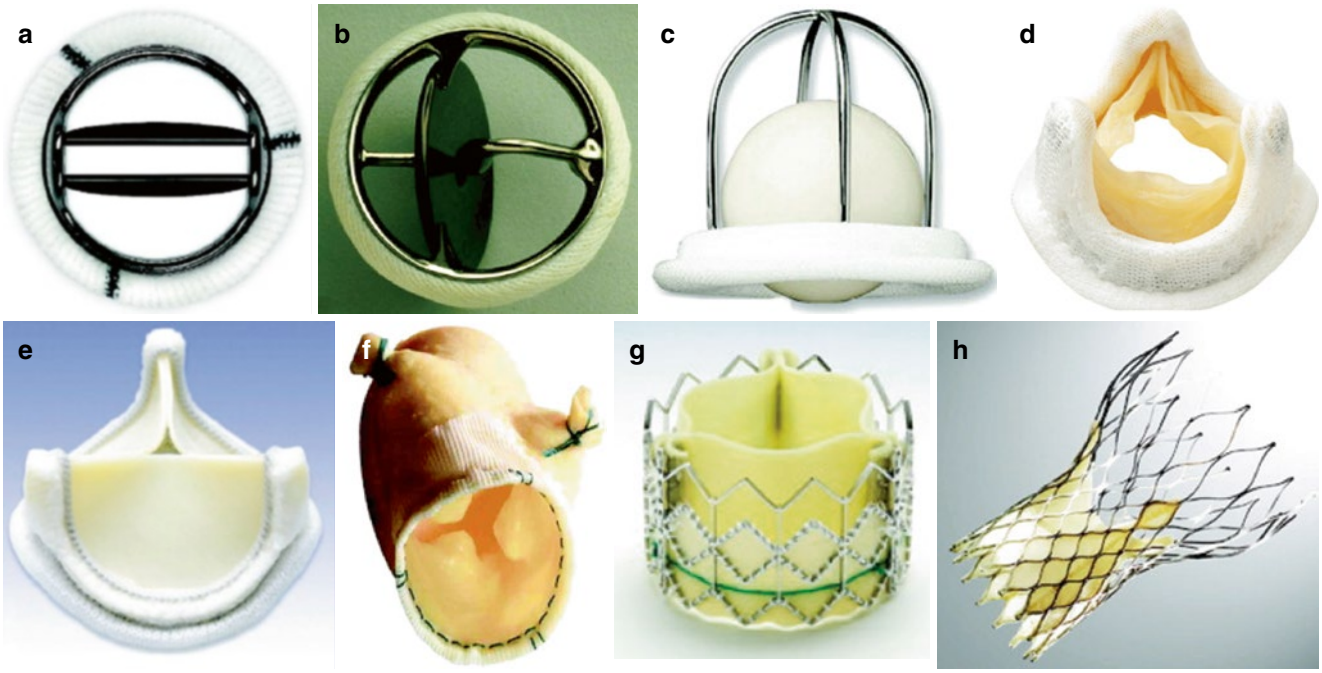

Fig. 16.15 Different types of prosthetic valves. (**a**) Bileaflet mechanical valve (St. Jude); (**b**) monoleaflet mechanical valve (Medtronic Hall); (**c**) caged ball valve (Starr-Edwards); (**d**) stented porcine bioprosthesis (Medtronic Mosaic); (**e**) stented pericardial bioprostheses (Carpentier-Edwards Magna); (**f**) stentless porcine bioprosthesis (Medtronic Freestyle); (**g**) percutaneous bioprosthesis expanded over a balloon (Edwards SAPIEN); (**h**) self-expandable percutaneous bioprosthesis (CoreValve). See text for details (*From Pibarot and Dumesnil* [95]*; with permission of Walters-Kluwer*)

are ever-present risks of thrombosis and endocarditis of the valve. In many types of mechanical valves, separate aortic and mitral versions are available; nonetheless for a number of the mechanical valves, implantation has been performed in any of the four valve positions.

Biologic heart valves are derived from human or animal tissue, and certain types contain nonbiologic material as well, such as metal and fabric. Human tissue valves fall into two categories: *homografts* (*allografts*) and *autografts*. Homograft valves are cryopreserved human cadaveric aortic and pulmonary valves, generally used as pulmonary or aortic valve replacements (Fig. 16.16). They come in a variety of sizes, depending upon donor availability. In contrast, an autograft represents the patient's own valve translocated from one site to another. Usually, the autograft is the patient's pulmonary valve translocated to the aortic position (Ross procedure) or rarely the mitral position (Ross II), with a homograft valve being placed in the original pulmonary position [86–88]. Biologic valves derived from animal tissue are known as *xenograft* (or *heterograft*) valves; the most commonly used animal tissues are porcine aortic valve and bovine pericardium, and the tissues are fixed with glutaraldehyde. These valves come in two major forms. *Stented* biologic valves contain a sewing ring and struts composed of nonbiologic material (metal, cloth), and valve tissue is sewn onto the fabric covering the struts. Both porcine valve (Fig. 16.15d) and bovine pericardium (Fig. 16.15e) are used with these types of valves. *Stentless* biologic valves contain no struts or sewing ring, which leaves more room for blood flow. Stentless xenograft valves derive primarily from harvested porcine aortic valves (Fig. 16.15f). Of note, human homograft and autograft valves also fall into the category of unstented biologic valves, since they contain no sewing ring or struts. This is because the entire homograft/allograft root (containing the valves) is harvested, thus the intrinsic structural support for the valve leaflets remains intact. Another category of bioprosthesis that has gained popularity is the Contegra pulmonary valve conduit. The Contegra conduit is a bovine jugular vein preserved in glutaraldehyde, and it contains a valve with three leaflets; the leaflets are similar to a human semilunar valve (Fig. 16.17). Since it is derived from a venous vascular structure, it is felt to be best suited for conditions of lower pressure such as the pulmonary circuit, and therefore it is used primarily for congenital heart surgeries in which a right ventricle to pulmonary artery conduit is needed such as the Ross procedure, tetralogy of Fallot, truncus arteriosus, etc. [89]. Thus it serves as an alternative to the homograft, and has achieved comparable short to intermediate term results [90–92]. Strictly speaking, it is a valved conduit (not solely a biologic valve), but it is used in a number of operations in which a valve is necessary. The Contegra conduit is available in both a supported and unsupported model;

the supported model contains two external cloth covered polypropylene rings that encircle the valve annulus and commissure to provide additional support (Fig. 16.17a), and is utilized in those cases in which sternal compression could be an issue. As will be discussed below, the bovine jugular valve is also used for transcatheter valve technology.

Over the years, a large number of different valve prostheses (both mechanical and biologic) have been developed, in a variety of valve sizes and profiles. Development continues at a rapid pace, with novel alternatives currently in development or advanced clinical trials. A list of some of the better-known biologic and mechanical valves is given in Table 16.6; this list is by no means exhaustive, and new models and types are periodically being introduced. A full discussion and elaboration of the many individual valves (including details about durability and complications) would require a separate chapter. For further information, the reader is referred to a number of references providing more detailed coverage of the topic [93–97].

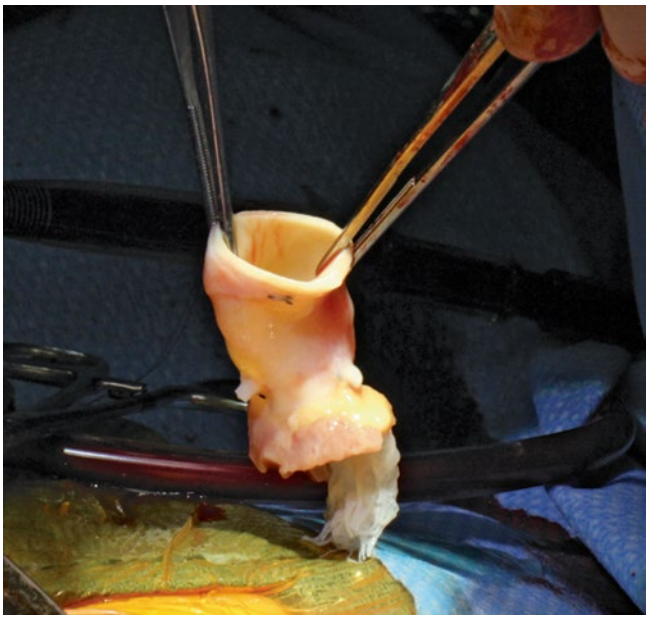

Fig. 16.16 Aortic homograft, following thawing and prior to implantation as a right ventricle to pulmonary artery conduit

Both mechanical and biologic valves can be used to replace a stenotic or regurgitant valve in any of the four valve positions. The preference for valve replacement type varies depending upon the desired site of implantation, and includes considerations such as age of the patient, evidence-based effectiveness of valve prosthesis alternatives for the intended valvar position, valve durability, valve size availability, and the need for ongoing medical therapy. Mechanical prostheses boast greater durability, but this must be balanced with the need for constant anticoagulation and the ever-present risks of bleeding, thrombosis, and endocarditis. Conversely, biologic valves do not generally require significant anticoagulation, but their durability can be much more variable. While there are multiple options for each valve site, some generalizations can be made [17]. For pulmonary valve replacement, biologic valves—notably homograft (allograft) and heterograft (porcine, bovine pericardial, contegra)—are generally preferred, though some investigators have advocated for mechanical valves [98]. For tricuspid, either a mechanical valve or stented porcine valve is generally used. For the aortic valve, both biologic (homograft, heterograft, pulmonary autograft) and mechanical prosthetic valves are utilized. A number of stented and unstented biosprosthetic xenograft valves have been developed for the aortic valve position. For the mitral valve, mechanical prostheses predominate in children and adults, although stented biologic valves (porcine and bovine pericardial) are selectively used in the adult group due to other important considerations (such as pregnancy and the risk of warfarin embryopathy) [17].

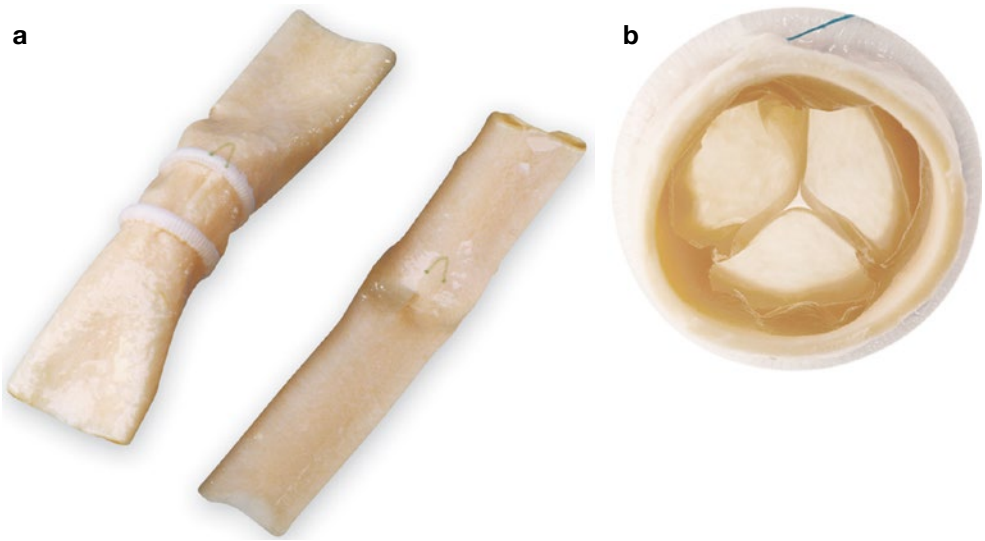

Fig. 16.17 Contegra pulmonary valve conduit. The Contegra conduit is a bovine jugular vein with a trileaflet valve that is similar to a human semilunar valve. (**a**) The conduit is available in supported and unsupported models. The supported model contains two external cloth covered polypropylene rings that encircle the valve annulus and commissure to provide additional support for the valve housed inside the conduit. (**b**) Cross-sectional *(en face)* view of the trileaflet bovine valve inside the conduit (Image published with permission from Medtronic, Inc)

Fig. 16.18 The Medtronic Melody transcatheter pulmonary valve consists of bovine jugular vein sutured in a 28 mm platinum-iridium stent. The valve is inserted using a 22 French balloon in balloon catheter delivery system (Ensemble) with a retractable sheath that covers the Melody valve once it is front loaded and crimped over the balloon (Reprinted from Fleming et al [99]; with permission from Elsevier)

One of the most important and exciting new areas in prosthetic valve technology has been the development of catheter-based, implantable prosthetic valves, also known as transcatheter heart valves or THVs. Valve leaflets composed of biologic tissue are mounted in an expandable metal frame, which can then be delivered using various transcatheter techniques and precisely placed in the location of the diseased or absent valve. Several of these THVs are well known, having already gained a large clinical experience. The **Melody valve** (Fig. 16.18) is a bovine jugular valve mounted on a platinum iridium stent, and delivered by a 22 F balloon in balloon catheter delivery system [99]. It is primarily designed for pulmonary valve replacement, and in the United States it is currently used only in an existing right ventricular outflow conduit, though in Europe it has also been used in patients with tetralogy of Fallot and a right ventricular outflow tract patch (using pre-stenting techniques) [100]. It has also been used in other positions such as failed AV valve bioprostheses (also known as "valve-in-valve" replacement) [99, 101, 102], native aortic valve replacement [101], and in the branch pulmonary arteries [103]. For transcatheter aortic valve replacement/implantation (also known as TAVR, or TAVI), there are two major devices currently available. The **Edwards SAPIEN** valve contains bovine pericardial leaflets sewn inside a stainless steel or cobalt chromium alloy frame. The inflow of the frame is covered with fabric to provide an

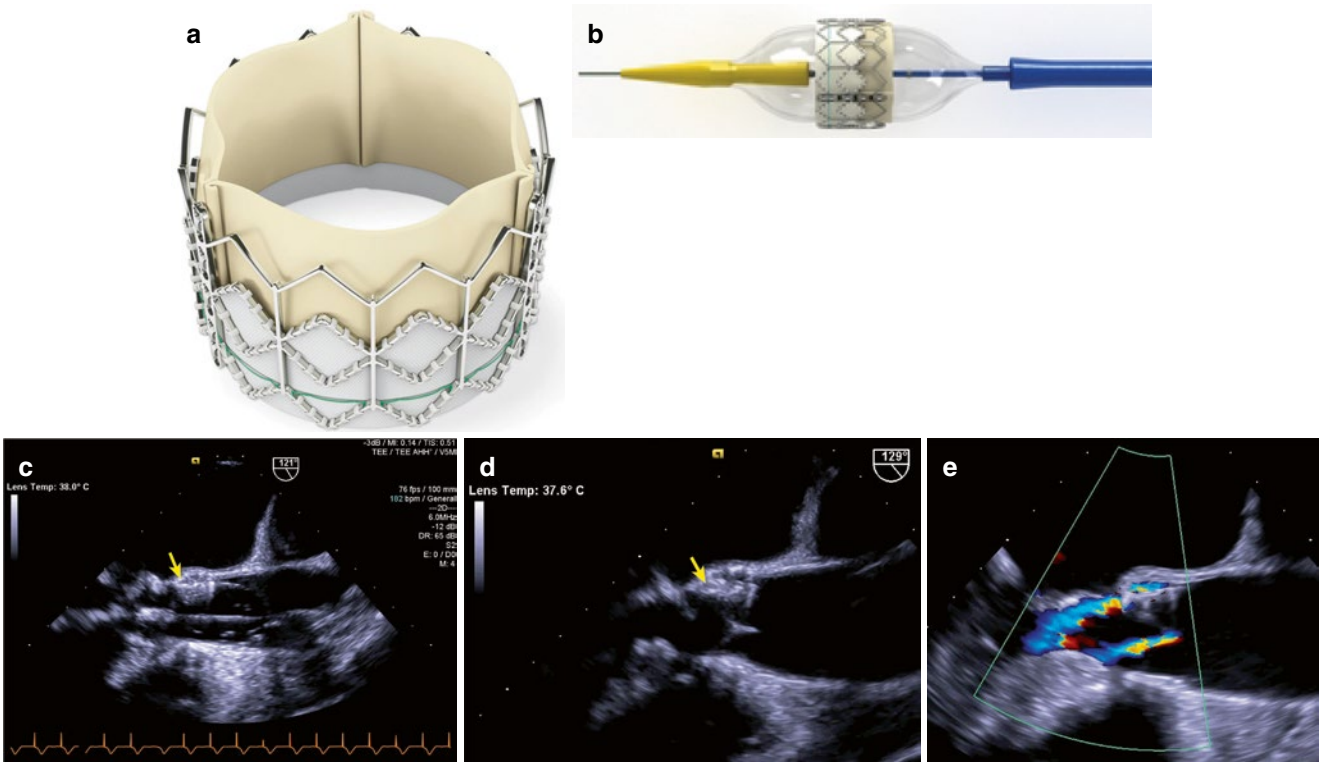

Fig. 16.19 Transcatheter aortic valve replacement/implantation (TAVR/TAVI). Figure **a** shows the Edwards SAPIEN valve (Edwards Lifesciences Inc., Irvine, California), a bovine pericardial valve mounted on a stainless steel frame. Figure **b** shows the same valve mounted on a balloon catheter that is used for valve delivery. Figure **c**–**e** are transesophageal echocardiographic images obtained from the mid esophageal aortic valve long axis view at 120°-130°. Figure **c** shows the balloon being inflated (device indicated with *arrow*), and figure **d** shows the valve (*arrow*) after implantation. In Figure **e**, following valve implantation color flow Doppler shows two small jets of regurgitation: one a central transvalvular jet, the other a peripheral paravalvular jet (Echocardiographic images were obtained from a Siemens SC 2000 platform and are courtesy of Siemens Medical Systems USA, Inc. © 2012–13 Siemens Medical Solutions USA, Inc. All Rights Reserved)

annulus seal (Figs. 16.15g and 16.19a, b). The valve is positioned through a sheath (22–24 F for the SAPIEN, 16–19 F for the SAPIEN XT) either from the femoral artery, ascending aorta, or through the left ventricular apex (the latter two methods utilizing a hybrid surgical approach). Once positioned, the frame and valve are balloon expanded within the diseased native aortic valve, displacing the native leaflets (Fig. 16.19). Rapid ventricular pacing is performed during implantation to reduce cardiac contraction during valve implantation [104]. This valve is also used for valve-in-valve replacement (mitral, tricuspid), and is undergoing trials for use in transcatheter pulmonary valve replacement (similar to the Melody valve) [99, 105]. The other major valve for TAVR/TAVI is the **Medtronic CoreValve** system. This valve is composed of porcine pericardial leaflets and annular seal, mounted in a self-expanding nitinol frame (Fig. 16.15h). It is delivered within an 18 F sheath, introduced percutaneously via femoral or subclavian artery access. Once the sheathed device is located in the desired position, the device expands (and becomes deployed) by retraction of the sheath. Deployment does not require rapid ventricular pacing. To date, it has limited utility for valve-in-valve therapy.

It should be noted that research and development in THVs continues at a very rapid pace; in the near future one can expect to see a number of new valves in various stages of clinical trials [106].

TEE Evaluation of Prosthetic Valves

Echocardiography is very important for the evaluation of both mechanical and biologic valves. This is particularly true in the intraoperative setting, in which TEE is used preoperatively to visualize the diseased valve location, size and pathology, and postoperatively to assess the function and anatomic appearance of the newly implanted prosthetic valve. However it is important to remember that the intraoperative setting presents unique challenges for valvar assessment due to physiologic alterations from changing preload/afterload, inotropic support, open sternum, positive pressure ventilation, and general anesthesia (also discussed in Chaps. 11 and 15).

The TEE evaluation of prosthetic valves utilizes the same principles applied to native valve pathology: one should

perform a combination of careful 2D imaging, as well as color flow and spectral Doppler evaluation of flow across the valve. For imaging, a prosthetic valve should be examined from multiple views, with emphasis on valve occluder/leaflet motion, appearance of the sewing ring, and presence of an abnormal echo density attached to any part of the prosthesis. The examiner should establish that the valve is well seated, and without excessive movement or "rocking", which could be a sign of dehiscence [107]. The imaging findings should always be paired with color flow and spectral Doppler evaluation, which gives important information regarding valve function, including possible paravalvar leaks as well as areas of stenosis/abnormal flow. The examiner should understand the type of prosthetic valve implanted, and whether there are any unique imaging/flow characteristics expected with that particular prosthesis. For example, imaging artifacts produced by certain prosthetic valves can sometimes interfere with their assessment. In this case the use of multiple imaging planes and views can help to circumvent these artifacts, and this is particularly applicable to TEE.

For mechanical prosthetic valves, echocardiography (both TTE and TEE) serves as an essential tool for evaluation [107]. Normal flow across a mechanical valve will be different than that of the corresponding native valve; increased spectral Doppler velocities can be anticipated, depending upon valve manufacturer and valve location and size. These "normal" or expected Doppler velocities have been well documented for the different valve types and sizes (discussed below) [95, 107, 108]. Mechanical valves can be difficult to image by TTE due to their nonbiologic material composition (metal and pyrolytic carbon) that produces significant acoustic shadowing and reverberation, as well as side lobe artifacts. As such, limited information is available in those areas of the valve prosthesis distal to the ultrasound transducer. Thus for certain mechanical valves, TEE can play a very important role in their evaluation because of the proximity of the TEE probe to the heart, with a location proximal to the prosthesis, resulting in superior overall imaging (Fig. 16.20). Excellent visualization of mechanical valve motion, as well as color flow and spectral Doppler evaluation can be obtained. Mechanical valves generally have flow characteristics that differ markedly from native valves. For example, the typical bileaflet tilting disk valve (e.g. St. Jude), when open, has one major central orifice and two side orifices to allow forward flow [95, 107]. When closed, there are normally two small regurgitant ("washing") jets at the pivot points of the valve, angled centrally; these are intended to minimize thrombus formation [109] (Fig. 16.21, Video 16.15). Abnormalities of valve occluder/leaflet motion (such as a frozen leaflet), vegetations, thrombus, pannus formation (tissue ingrowth at the site of the valve prosthesis), and paravalvar leaks/valve dehiscence, can all be seen well by TEE [94, 109]. For mechanical prosthetic valve endocarditis, TEE has been shown to be clearly superior to TTE: vegetations and annular abscesses can be visualized much more readily [41, 110–112]. With mechanical prostheses, vegetations can significantly interfere with occluder motion, causing stenosis, regurgitation, or both [109].

With mechanical AV valve evaluation, TEE can very useful. This is especially true with mechanical mitral valves, in which the superiority of TEE imaging compared to TTE is most striking. The esophageal position of the TEE probe enables imaging of the important atrial surface of the valve—an area where pathology tends to occur, often obscured by standard TTE. Excellent valve detail is obtainable from the mid esophageal window: rotation of the multiplane angle can be performed between 0° and 90° to provide optimal visualization of the prosthesis leaflets and leaflet motion from an edge-on view (particularly for bileaflet tilting valves). Restricted leaflet motion and pannus/vegetations above the valve can be very well seen (Figs. 16.22 and 16.23, Videos 16.16 and 16.17). One other important issue to note is that the native papillary muscles and chordal tissue can sometimes be left in place following AV valve replacement, and the chordae can remain quite mobile during the cardiac cycle. These structures should not be confused with intracardiac masses or thrombi.

Mechanical aortic valves can be more challenging to evaluate, as the mid esophageal plane of imaging tends to be parallel to the plane of the valve, and therefore more perpendicular to the direction of valve flow. Depending upon valve leaflet orientation, it might be difficult to obtain an edge-on profile of leaflet motion. Instead, often the leaflets can be viewed from an *en face* perspective. They can be examined for any asymmetry of motion, and any paravalvar leaks can be viewed from a number of different multiplane angles between 0°–120° (Fig. 16.3, Video 16.3). If transgastric and deep transgastric views are available, these can be particularly useful to evaluate the proximal (subaortic) portion of the valve, visualize valve motion, evaluate for valvar regurgitation, and also obtain a spectral Doppler tracing across the valve [109] (Fig. 16.24, Video 16.18). These latter transducer positions help to avoid the shadowing artifacts associated with imaging from the mid esophageal position.

Biologic prosthetic valves—both stented and stentless—generally have much less acoustic shadowing, and are therefore seen more readily both by TTE and TEE (Fig. 16.25a, b). The struts of a stented valve are echogenic and easily seen arching above the plane of the valve ring; however the thin valve leaflets should be seen contained within the valve (Fig. 16.25a). Stentless valves (homograft, xenograft, autograft) often have an echocardiographic appearance similar to that of native valve tissue (Fig. 16.25b). Biologic prosthetic valve motion and valve characteristics are generally seen very well by echocardiography. Unlike mechanical valves, these valves do not incorporate valve regurgitation as part of their design. However, very minor degrees of regurgitation

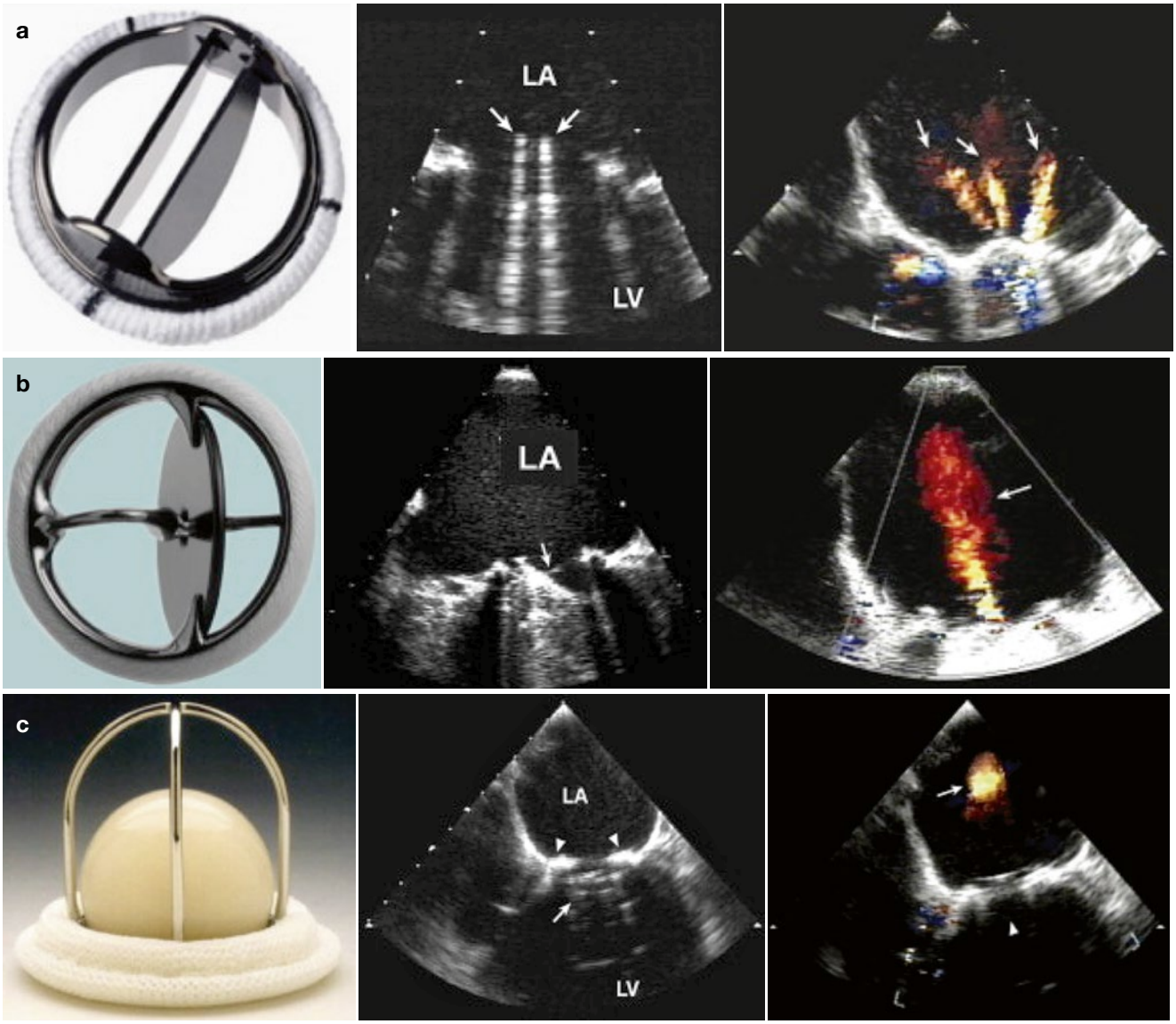

Fig. 16.20 Examples of bileaflet (St. Jude, **a**), single-leaflet (Medtronic-Hall, **b**), and caged-ball (Starr-Edwards, **c**) mechanical valves and their transesophageal echocardiographic characteristics taken in the mitral position in diastole (*middle*) and in systole (*right*). The *arrows* in diastole point to the occluder mechanism of the valve and in systole to the characteristic physiologic regurgitation observed with each valve. In Figure 16c, the *arrowheads* in the middle photograph indicate the valve sewing ring, and in the right photograph the caged ball occluding the valve. (Reprinted from: Zoghbi et al [107]; with permission from Elsevier)

are normally present in many patients [109]. Valve failure (stenosis and/or regurgitation) is readily seen and evaluated both by TTE and TEE, using imaging, color flow and spectral Doppler. Since TTE is adequate for most biologic valves, TEE is usually reserved for those patients in whom TTE imaging is suboptimal, in patients suspected of having endocarditis (see above), or in the intraoperative setting. One of the more useful aspects of the postoperative TEE study following prosthetic valve implantation (both biologic and mechanical) is to establish the flow profile across the new valve; this information (including velocities) can be used for subsequent comparisons.

Doppler Evaluation of Prosthetic Valves

For Doppler evaluation of prosthetic valves, the principles and techniques of valve interrogation and recording of flow velocity are similar to those used for evaluating native valve stenosis or regurgitation (see Chaps. 8 and 11) [113, 114]. However a few general comments are worth noting. Prosthetic valve regurgitation is primarily assessed with Doppler evaluation, mainly using color flow techniques, though spectral Doppler evaluation is helpful as well. It is important to differentiate between "normal" and pathologic prosthetic valve regurgitation. A mild degree of

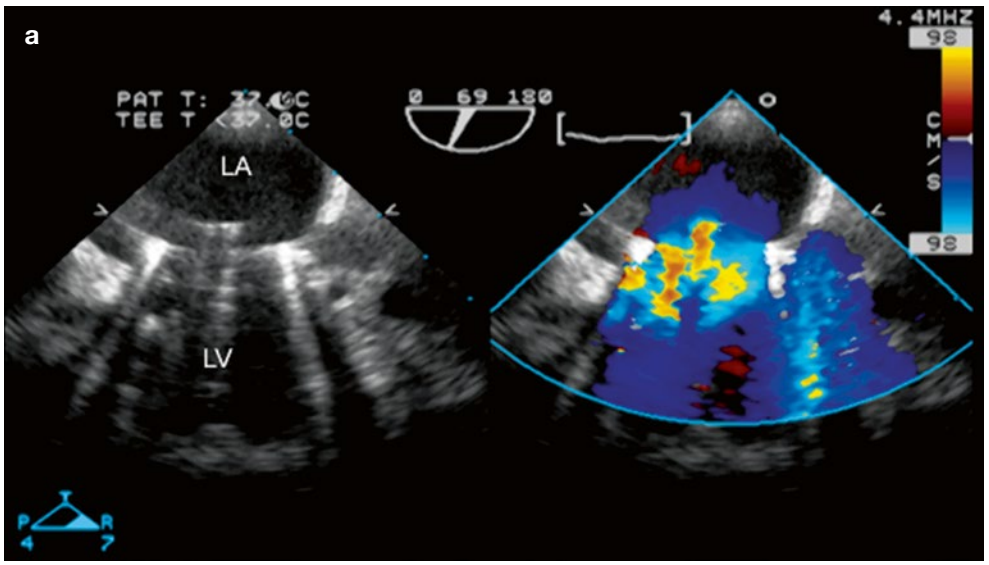

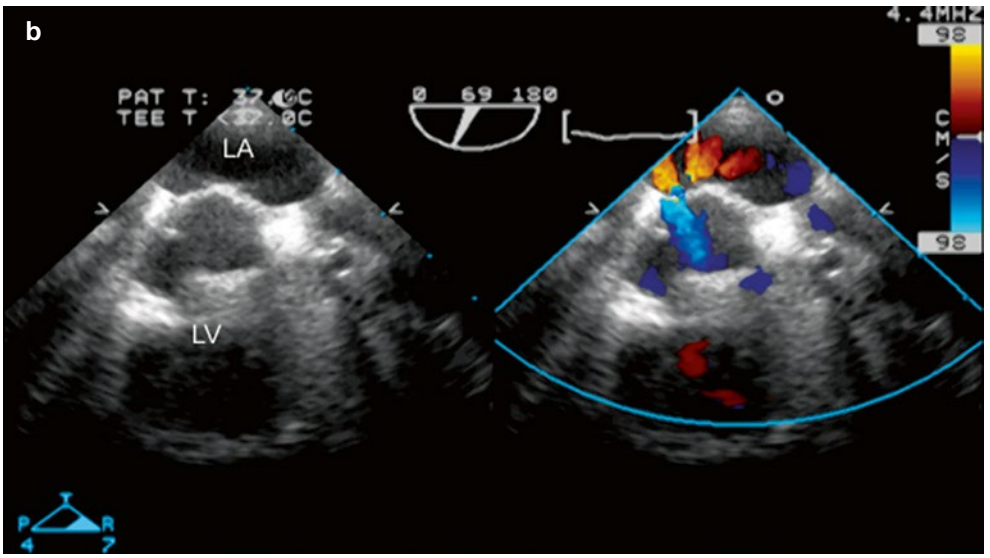

Fig. 16.21 Prosthetic mitral valve (St Jude bileaflet disk). Mid esophageal view mitral commissural view, multiplane angle 69°. The multiplane angle is rotated until both leaflets are profiled and open symmetrically in diastole (**a**) and systole (**b**). (**a**) There is the usual color flow Doppler profile across the valve (*see* text for details). (**b**) In systole, the "normal" pivot point washing jets are seen. *LA* left atrium, *LV* left ventricle

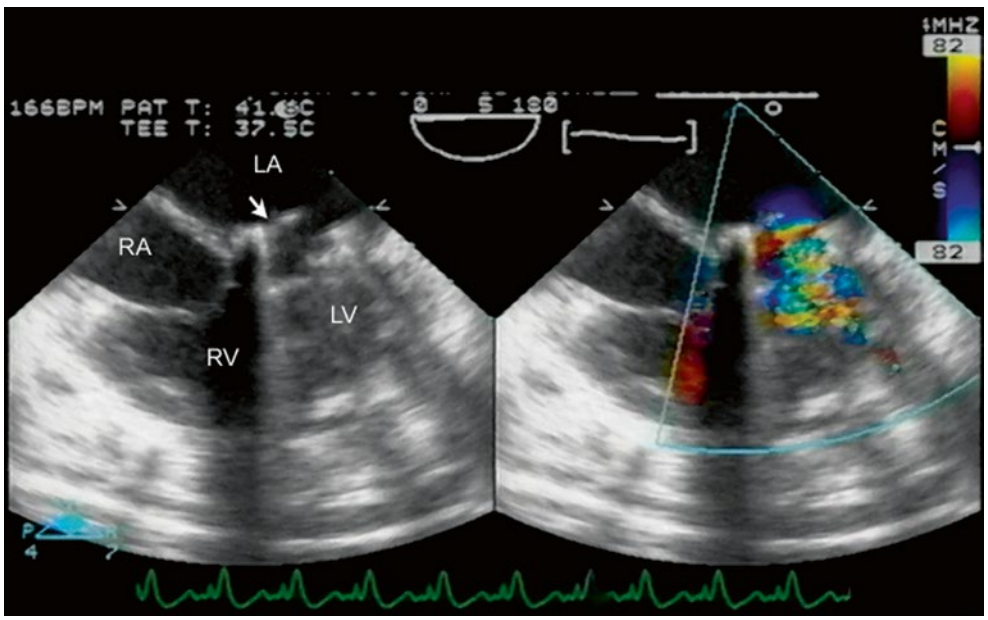

Fig. 16.22 Prosthetic mitral with a frozen leaflet (*arrow*), causing stenosis of the valve, seen as color flow Doppler aliasing in the right panel. Mid esophageal four chamber view, multiplane angle 0°. *LA* left atrium, *LV* left ventricle, *RA* right atrium, *RV* right ventricle

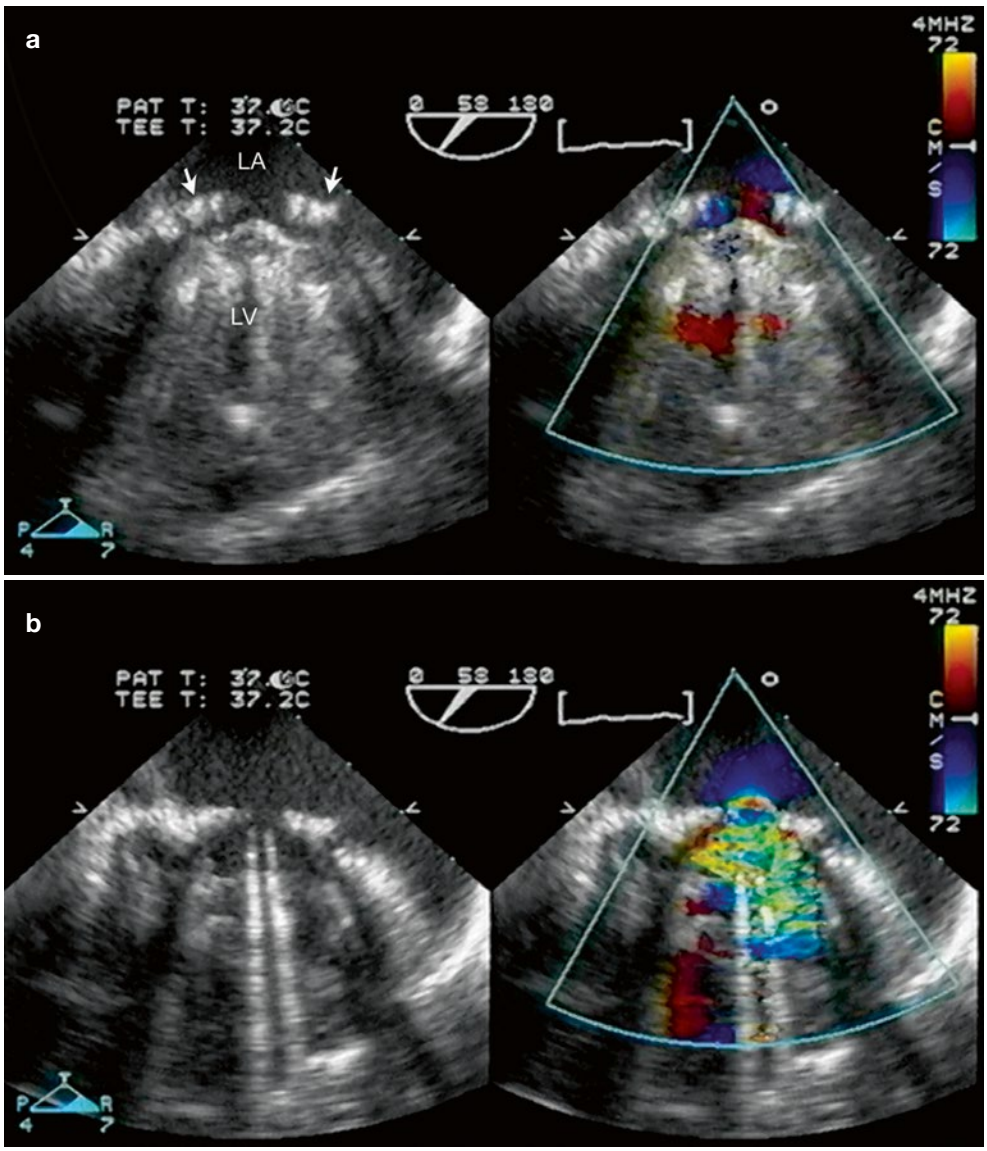

Fig. 16.23 Concentric pannus formation (*arrows*) above the mitral valve prosthesis (**a**), causing significant supravalvar narrowing, seen during diastole (**b**). In **b**, note the color flow Doppler aliasing that begins above the prosthetic valve, at the level of the pannus. Mid esophageal mitral commissural view, multiplane angle 58°. *LA* left atrium, *LV* left ventricle

regurgitation is normally seen in virtually all mechanical valves (Fig. 16.20); as noted above, this can be seen in the form of the "washing" jets seen with bileaflet valves (Fig. 16.21, Video 16.15). Minor regurgitant jets are also seen with biologic valves, including THVs. Pathologic regurgitation—characterized as one or more prominent areas of color flow Doppler regurgitation—can be either central or paravalvular (outside the valve sewing ring). Most pathologic central regurgitation is seen in biologic valves, but paravalvular regurgitation can occur with both biologic and mechanical valves. Paravalvular regurgitation is seen as jets outside the sewing ring of the prosthesis (Fig. 16.26, Video 16.19). The degree of regurgitation can be estimated using the methods for quantification of native valvular regurgitation [113], although these can be more challenging with the shadowing and reverberations caused by the prosthetic valves (particularly mechanical valves). Commonly used parameters for semilunar valves include color flow Doppler jet width, vena contracta, pressure half-time, and diastolic flow reversal in the distal great artery; for AV valves, parameters include vena contracta, color flow Doppler jet area, as well as reversal of flow in the pulmonary or systemic veins. A discussion of this evaluation is given in Chaps. 8 and 11. Regardless of valve type and position, when pathologic regurgitation is suspected, a careful evaluation must be made as to possible etiology. This includes location of the regurgitation (central vs. paravalvular), and possible mechanism of regurgitation (leaflet dysfunction, improper valve size/geometric mismatch, valve dehiscence, etc.).

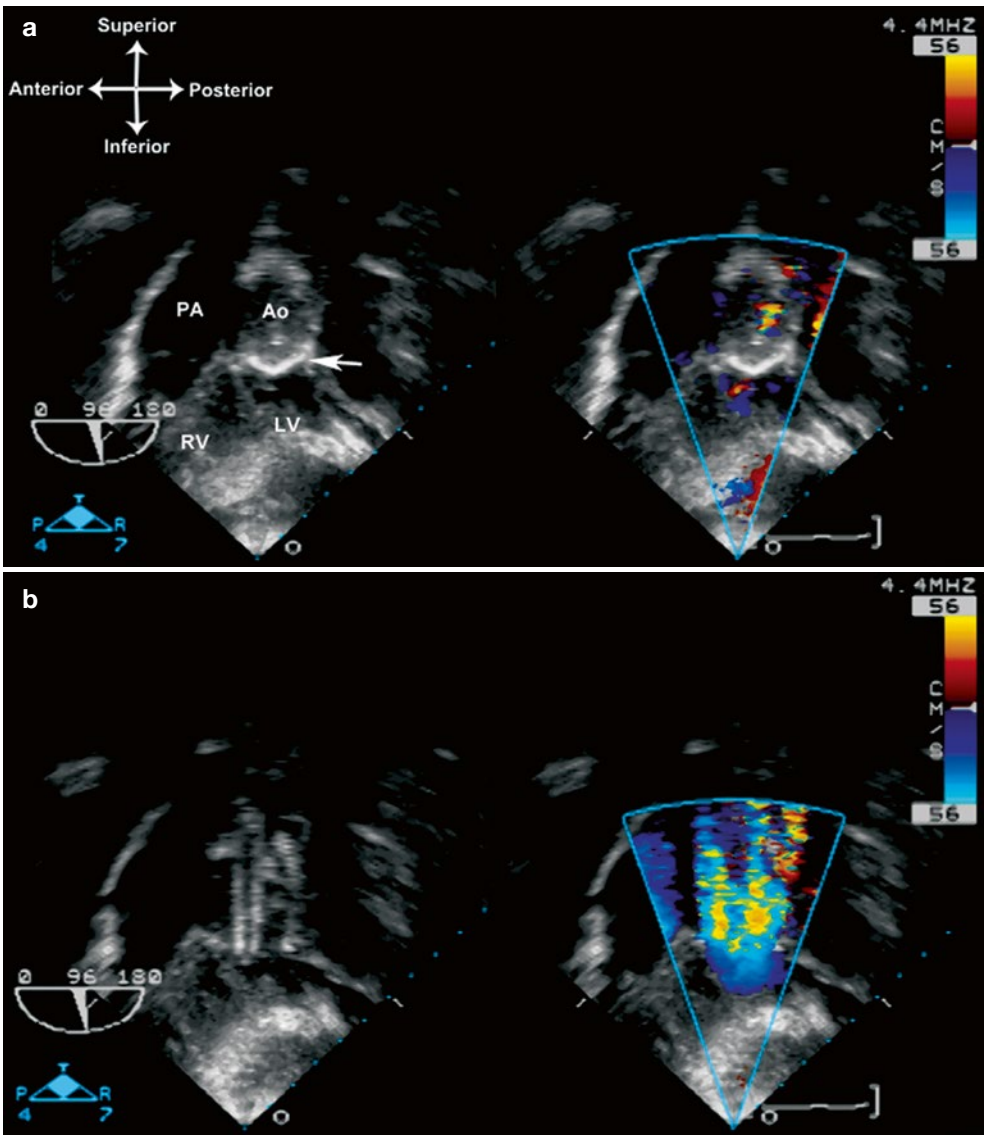

Fig. 16.24 Prosthetic aortic valve (bileaflet tilting disk) viewed from deep transgastric position, multiplane angle 96°. The multiplane angle has been rotated until both leaflets are profiled and symmetric leaflet motion is noted in diastole (**a**) and systole (**b**). The prosthetic valve position is marked by the *arrow*. This transducer position affords a good view of leaflet motion and flow across the valve, and also provides an excellent angle for spectral Doppler evaluation. *Ao* ascending aorta, *LV* left ventricle, *PA* pulmonary artery, *RV* right ventricle

When evaluating antegrade flow across prosthetic valves, it is important to remember that the flow characteristics and velocities across prosthetic valves (particularly mechanical valves) will often differ from comparably sized native valves. In general, the spectral Doppler velocities across these valves tend to be higher due to the phenomenon of pressure recovery [107]. As mentioned above, several studies have presented expected Doppler velocities, gradients and effective orifice area for a wide range of biologic and mechanical aortic and mitral valves [95, 107, 108]. Tables 16.7 and 16.8 show representative data abstracted from one of these studies [108] for several common prosthetic aortic and mitral valves. It should be noted that the labeled valve "size" (e.g. 21, 23 mm) represents the outer valve diameter in millimeters as given by the manufacturer. However this parameter should not be considered alone, because the flow characteristics and cross-sectional area between two identically sized valves might be completely different. Hence the effective orifice area (EOA) presented in these tables represents a better parameter for valve comparisons and overall prosthetic valve evaluation; it is an important parameter utilized in adult patients for clinical prosthetic valve assessment. The EOA is analogous to valve orifice area for a native valve, and is calculated in the same manner by the continuity equation (Chap. 1):

$$\textbf{EOA} = \textbf{Stroke volume} / \textbf{VTI}_{\textbf{PrV}}$$

VTI_{PrV} = Velocity time integral (VTI) through the prosthesis, measured by continuous wave Doppler

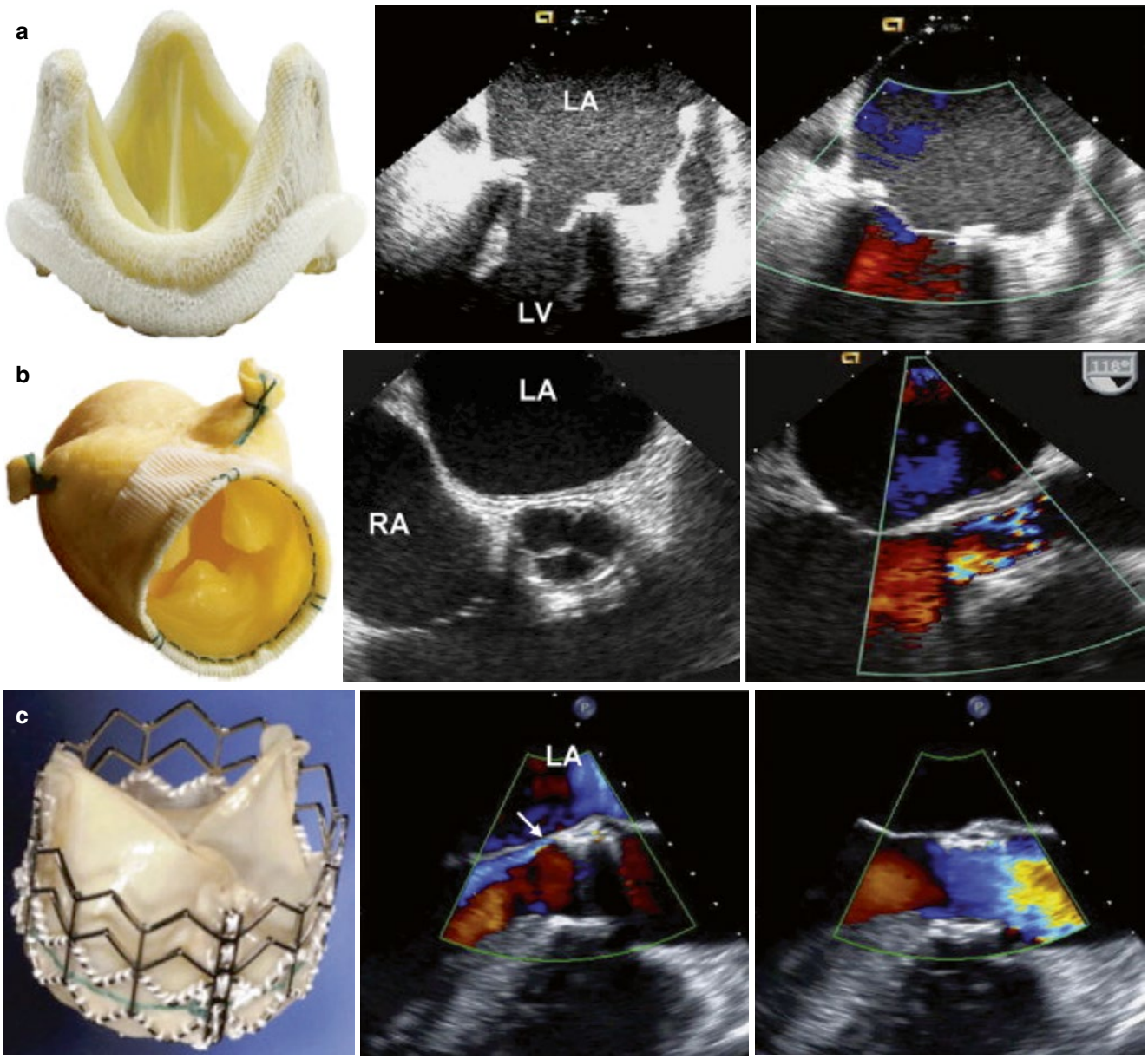

Fig. 16.25 Examples of stented (**a**), stentless (**b**), and percutaneous biologic valves (Edwards SAPIEN, **c**) and their echocardiographic features in diastole (*middle*) and in systole (*right*) as seen by TEE. The stentless valve is inserted by the root inclusion technique. Mild paravalvular aortic regurgitation in the percutaneous valve is shown by *arrow* (From: Zoghbi et al [107]; with permission from Elsevier)

Stroke volume = VTI of the left ventricular outflow tract (by pulsed wave Doppler) multiplied by the left ventricular outflow tract cross sectional area (with prosthetic mitral valves, this calculated stroke volume is valid assuming no significant aortic regurgitation exists).

The EOA is generally a better index of valve function than gradient alone, because it is will not vary with different flow states. An important concept for prosthetic valves is that the EOA must be appropriate for the flow requirements of the individual, otherwise *patient-prosthetic mismatch* (PPM) occurs. PPM is a term used to describe the clinical situation when the EOA of a prosthetic valve is too small in relation to a patient's body size, resulting in abnormally high postoperative gradients [95, 115]. Studies in adults have shown that aortic PPM is associated with worsening

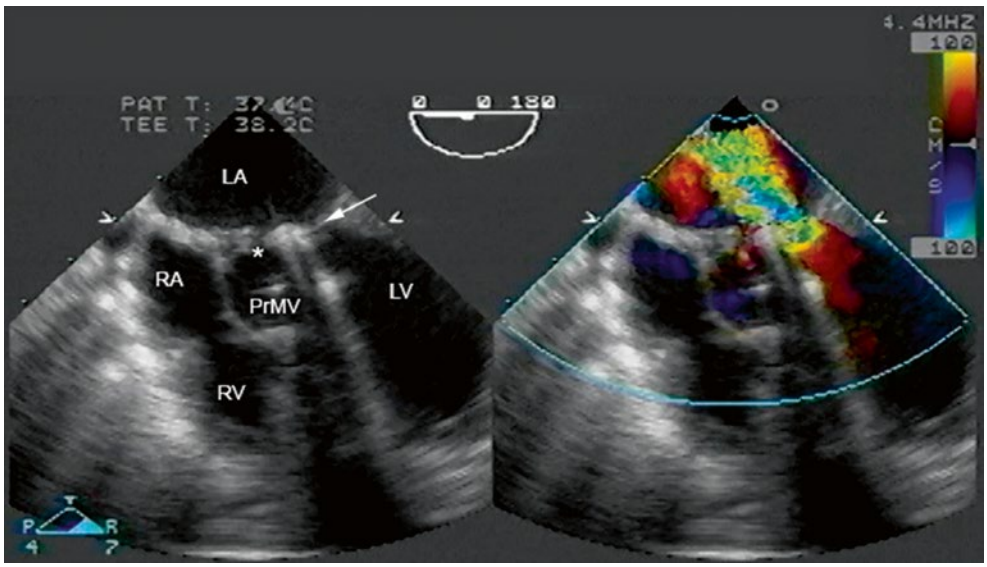

Fig. 16.26 Paravalvar regurgitation in a child who underwent mitral valve replacement with a mechanical bileaflet prosthesis (the patient previously underwent repair of an atrioventricular septal defect). This image was obtained from a mid esophageal four chamber view. The prosthesis was too large for the annulus and required insertion at an angle, which resulted both in a large area of paravalvular regurgitation (*arrow*) as well as a very small effective orifice (*asterisk*). *LA* left atrium, *LV* left ventricle, *PrMV* prosthetic mitral valve, *RA* right atrium, *RV* right ventricle

symptoms and impaired exercise capacity, as well as adverse cardiac events and long-term mortality [116–119]; mitral PPM is associated with persisting pulmonary hypertension and increased congestive heart failure as well as reduced survival [120]. When indexed to body surface area, the EOA is the only parameter found to be consistently related to postoperative gradients and/or adverse clinical outcomes [121–123]. Table 16.9 shows threshold values for indexed EOA generally used to identify and quantify the severity of PPM in adults [95].

As noted above, the information from Tables 16.7 and 16.8 are derived from studies in which data were compiled from a number of adult studies. The tables are voluminous and comprehensive, and the reader is referred to these for further reference regarding other prosthetic valves. Nonetheless, from these data, some simplified general guidelines can be formulated to assist in the assessment of possible prosthetic aortic and mitral valve stenosis, and these are summarized by Zoghbi et al [107] and presented in Table 16.10. These guidelines also utilize parameters such as Doppler velocity index (DVI) for prosthetic aortic valves, which is the ratio of velocities across the left ventricular outflow tract compared to the velocity across the prosthetic aortic valve, and the inverse relationship for mitral valves, the ratio of the prosthetic mitral valve VTI compared to the VTI across the left ventricular outflow tract. These dimensionless ratios—derived from the continuity equation—are much less dependent upon varying flow states. It should be noted that comparable data for prosthetic pulmonary and tricuspid valves is lacking, particularly regarding normal and abnormal EOAs and DVI/VTI. Therefore more general guidelines, also presented by Zoghbi et al, have been presented for these latter two valves as follows [107]:

- Findings suspicious for prosthetic pulmonary stenosis:
  - Cusp or leaflet thickening or immobility.
  - Narrowing of forward color map.
  - Peak velocity through the prosthesis >3 or >2 m/s through a homograft (suspicious but not diagnostic of stenosis).
  - Increase in peak velocity on serial studies (more reliable parameter).
  - Impaired right ventricular function or elevated right ventricular systolic pressure.
- Findings suspicious for tricuspid valve stenosis
  - Peak velocity >1.7 m/s (because of respiratory variation, average ≥5 cycles).
  - Mean gradient ≥6 mmHg (may be increased if there is valvular regurgitation).
  - Pressure half-time ≥230 ms.
  - Narrow inflow color map.
  - Nonspecific signs such as enlarged right atrium and engorged inferior vena cava.

In general, an integrated approach, using a combination of the criteria discussed above, works best when evaluating forward flow across any prosthetic valve.

For pediatric patients, there is a notable paucity of available published information regarding normal velocities and EOAs across prosthetic valves, particularly the smaller mitral and aortic valves. Much of the information used in the pediatric population originates from adult data. Fortunately many of the same principles can still be applied, though comparable values to those obtained in adults are still lacking, and it is unclear whether certain parameters are

equivalent in this group of patients. For example, one study evaluating St. Jude and Carbomedics mitral prostheses in children found that peak early Doppler velocity—not EOA—correlated best with the manufacturer's geometric valve orifice area, and also pulmonary artery wedge pressure [124]. The use of the DVI and VTI ratios has not been established in the pediatric population. Also, PPM has not been evaluated closely in children, though it would seem evident that

Table 16.7 Doppler parameters across prosthetic aortic valves

Valve	Size (mm)	Peak gradient (mmHg)	Mean gradient (mmHg)	Peak velocity (m/s)	Effective orifice area (cm^2)
Stented biologic					
Hancock II (porcine)	21	20±0.4	14.8±4.1		1.23±0.3
	23	24.7±5.7	16.6±6.9		1.39±0.2
	25	20±2	10.7±3		1.47±0.2
	27	14±3			1.55±0.2
	29	15±3			1.6±0.2
Mosaic (porcine)	21		12.4±7.3		1.6±0.7
	23		12.5±7.4		2.1±0.8
	25		10.1±5.1		2.1±1.6
	27		9.0		1.8±0.4
	29		9.0		2.0±0.4
Carpentier-Edwards (pericardial)	19	32.1±3.4	24.2±8.6	2.8±0.1	
	21	25.7±9.9	20.3±9.1	2.6±0.4	1.2±0.3
	23	21.7±8.6	13.0±5.3	2.3±0.5	1.5±0.4
	25	16.5±5.4	9.0±2.3	2.0±0.3	1.8±0.3
	27	19.2±0	5.6	1.6	2.1±0.4
	29	17.6±0	11.6	2.1	2.2±0.4
Mitroflow (pericardial)	19	18.7±5.1	10.3±3		1.1±0.1
	21	20.2	15.4	2.3	1.3±0.1
	23	14.0±4.9	7.6±3.4	1.9±0.3	1.5±0.2
	25	17±11.3	10.8±6.5	2±0.7	1.8±0.2
	27	13±3	6.6±1.7	1.8±0.2	
Stentless biologic					
Medtronic Freestyle	19		13.0		
	21		8±2.6		1.6±0.3
	23		7.2±2.5		1.9±0.5
	25		5.4±1.5		2.0±0.4
	27		4.7±1.6		2.5±0.5
St. Jude Toronto SPV	21	18.6±11.8	7.6±4.4		1.2±0.7
	23	13.6±7.3	7.1±4.3		1.6±0.8
	25	12.2±5.8	6.2±3.1		1.6±0.4
	27	10±4.6	4.8±2.3		2±0.4
	29	7.9±4.2	3.9±2.2		2.4±0.7
Mechanical					
Medtronic-Hall	20	34.4±13.1	17.1±5.3	2.9±0.4	1.21±0.45
	21	26.9±10.5	14.1±5.9	2.4±0.4	1.08±0.17
	23	26.9±8.9	13.5±4.8	2.4±0.6	1.36±0.39
	25	17.1±7.0	9.5±4.3	2.3±0.5	1.9±0.47
	27	18.7±9.7	8.7±5.6	2.1±0.5	1.9±0.16
	29			1.6	
Carbomedics (bileaflet)	17	33.4±13.2	20.1±7.1	—	1.02±0.2
	19	33.3±11.2	11.6±5.1	3.1±0.4	1.25±0.4
	21	26.3±10.3	12.7±4.3	2.6±0.5	1.42±0.4
	23	24.6±6.9	11.3±3.8	2.4±0.4	1.69±0.3
	25	20.3±8.7	9.3±4.7	2.3±0.3	2.04±0.4
	27	19.1±7.0	8.4±2.8	2.2±0.4	2.55±0.3
	29	12.5±4.7	5.8±3.2	1.9±0.3	2.63±0.4

Table 16.7 (continued)

Valve	Size (mm)	Peak gradient (mmHg)	Mean gradient (mmHg)	Peak velocity (m/s)	Effective orifice area (cm^2)
St. Jude (bileaflet)	19	35.2 ± 11.2	19 ± 6.2	2.9 ± 0.5	1.01 ± 0.2
	21	28.3 ± 9.9	15.8 ± 5.7	2.6 ± 0.5	1.33 ± 0.3
	23	25.3 ± 7.9	13.8 ± 5.3	2.6 ± 0.4	1.6 ± 0.4
	25	22.6 ± 7.7	12.7 ± 5.1	2.4 ± 0.5	1.93 ± 0.45
	27	19.9 ± 7.6	11.2 ± 4.8	2.2 ± 0.4	2.35 ± 0.6
	29	17.7 ± 6.4	9.9 ± 2.9	2 ± 0.1	2.81 ± 0.6
	31	16.0	10 ± 6	2.1 ± 0.6	3.08 ± 1.1
On-X (bileaflet)	19	21.3 ± 10.8	11.8 ± 3.4	—	1.5 ± 0.2
	21	16.4 ± 5.9	9.9 ± 3.6	—	1.7 ± 0.4
	23	15.9 ± 6.4	8.5 ± 3.3	—	2.0 ± 0.6
	25	16.5 ± 10.2	9 ± 5.3	—	2.4 ± 0.8
	27–29	11.4 ± 4.6	5.6 ± 2.7	—	3.2 ± 0.6
Starr-Edwards (Ball and Cage)	21	29			1.0
	23	32.6 ± 12.8	22 ± 8.8	4 ± 0	
	24	34.1 ± 10.3	22 ± 7.5	3.5 ± 0.5	1.1
	26	31.8 ± 9.0	19.7 ± 6.1	3.4 ± 0.5	
	27	30.8 ± 6.3	18.5 ± 3.7	3.2 ± 0.4	1.8
	29	29 ± 9.3	16.3 ± 5.5		

Table abstracted from Rosenhek et al [108]; with permission from Elsevier

Table 16.8 Doppler parameters across prosthetic mitral valves

Valve	Size (mm)	Peak gradient (mmHg)	Mean gradient (mmHg)	Peak velocity (m/s)	Pressure half-time (ms)	Effective orifice area (cm^2)
Stented biologic						
Hancock II (porcine)	27					2.2 ± 0.14
	29					2.8 ± 0.11
	31					2.8 ± 0.1
	33					3.2 ± 0.2
Carpentier-Edwards (pericardial)	27		3.6	1.6		
	29		5.3 ±3.4	1.7 ± 0.3		
	31		4 ± 0.8	1.5 ± 0.1		
	33		1.0	0.8		
Mitroflow (pericardial)	25		6.9	2.0	90	
	27		3.1 ± 0.9	2.5	90 ± 20	
	29		3.5 ± 1.7	1.4 ± 0.3	102 ± 21	
	31		3.9 ± 0.8	1.3 ± 0.3	91 ± 22	
Mechanical						
Carbomedics (bileaflet)	23			1.9 ± 0.1	126 ± 7	
	25	10.3 ± 2.3	3.6 ± 0.6	1.3 ± 0.1	93 ± 8	2.9 ± 0.8
	27	8.8 ± 3.5	3.5 ± 1.0	1.6 ± 0.3	89 ± 20	2.9 ± 0.8
	29	8.8 ± 2.9	3.4 ± 1.0	1.5 ± 0.3	88 ± 17	2.3 ± 0.4
	31	8.9 ± 2.3	3.3 ± 0.9	1.6 ± 0.3	92 ± 24	2.8 ± 1.1
	33	8.8 ± 2.2	4.8 ± 2.5	1.5 ± 0.2	93 ± 12	
St Jude (bileaflet)	23		4	1.5	160	1.0
	25		2.5 ± 1	1.3 ± 1.2	75 ± 4	1.4 ± 0.2
	27	11 ± 4	5 ± 1.8	1.6 ± 0.3	75 ± 10	1.7 ± 0.2
	29	10 ± 3	4.2 ± 1.8	1.6 ± 0.3	85 ± 10	1.8 ± 0.2
	31	12 ± 6	4.5 ± 2.2	1.6 ± 0.3	74 ± 13	2.0 ± 0.3

(continued)

Table 16.8 (continued)

Valve	Size (mm)	Peak gradient (mmHg)	Mean gradient (mmHg)	Peak velocity (m/s)	Pressure half-time (ms)	Effective orifice area (cm^2)
On-X (bileaflet)	25	11.5 ± 3.2	5.3 ± 2.1			1.9 ± 1.1
	27–29	10.3 ± 4.5	4.5 ± 1.6			2.2 ± 0.5
	31–33	9.8 ± 3.8	4.8 ± 2.4			2.5 ± 1.1
Starr-Edwards (Ball and Cage)	26		10			
	28		7 ± 2.8			
	30	12.2 ± 4.6	7 ± 2.5	1.7 ± 0.3	125 ± 25	1.7 ± 0.4
	32	11.5 ± 4.2	5.1 ± 2.5	1.7 ± 0.3	110 ± 25	2 ± 0.4
	34		5			

Table abstracted from Rosenhek et al [108]; with permission from Elsevier.

this particular parameter has direct relevance in the pediatric population because of growth considerations. While the goal for valve replacement in children is to implant the largest possible prosthesis, patient growth will inevitably lead to some degree of PPM, even with a normally functioning prosthesis [107]. As noted above, the most widely accepted and validated parameter for identifying PPM in adult patients is the indexed EOA, and Table 16.9 shows threshold values for indexed EOA generally used to identify and quantify the severity of PPM in adults [95]. This table might also serve as useful guide in children, although the applicability of these values in pediatrics has yet to be fully determined.

Table 16.9 Threshold values of indexed prosthetic valve effective orifice area (EOA) for the identification and quantification of prosthesis-patient mismatch

	Mild or not clinically significant (cm^2/m^2)	Moderate (cm^2/m^2)	Severe (cm^2/m^2)
Aortic position	>0.85 (0.8–0.9)	≤0.85 (0.8–0.9)	≤0.65 (0.6–0.7)
Mitral position	>1.2 (1.2–1.3)	≤1.2 (1.2–1.3)	≤0.9 (0.9)

From Pibarot and Dumesnil [95]; with permission of Walters-Kluwer
Numbers in parentheses represent the range of threshold values that have been used in the literature

TEE Evaluation of Transcatheter Heart Valve Implantation

For catheter-based implantable heart valves, the role of TEE will vary based upon the type of THV and its position. With TAVR/TAVI (both SAPIEN and CoreValve), TEE plays an integral role in all three phases of the procedure: preprocedural assessment of morphology and annular measurements, intraprocedural monitoring of all phases of the valve implantation (including guide wire and device positioning and valve deployment), and post-deployment assessment of possible paravalvular device leaks as well as ventricular function, mitral valve assessment, pericardial effusion, and aortic dissection [125, 126]. It is not uncommon to see some paravalvular regurgitation following valve implantation, particularly after TAVR/TAVI. An example of TEE monitoring during TAVR/TAVI (SAPIEN valve) is shown in Fig. 16.19, Video 16.20 (also in Chap. 11). For the Melody valve, TEE is generally not performed during valve implantation, though transthoracic imaging is routinely obtained after the procedure to assess valve function and competence. For valve-in-valve implantation, the role of TEE will vary depending upon the fluoroscopic visibility of the biologic valve. In most cases, when a stented bioprosthesis is readily visible on fluoroscopy, TEE might not be necessary. However in those cases in which the bioprostheses is not readily visible, or assessment of valve function is required, TEE can be very helpful [102].

Evaluation of Heart Transplantation/ Ventricular Assist Devices

Management of heart transplant recipients requires ongoing cardiac assessment for rejection and cardiac function, and this necessitates both noninvasive and invasive surveillance using echocardiography and cardiac catheterization/myocardial biopsy. The bulk of noninvasive surveillance is provided primarily by TTE; the use of TEE for heart transplantation is generally confined to the immediate pre-transplant and post-transplant period. The specific applications for TEE in the setting of heart transplantation include the following:

- *Screening of cardiac transplant donors*. Echocardiography is an essential part of the evaluation of any prospective cardiac transplant donor. Cardiac function and segmental wall motion must be assessed, and any potential intracardiac abnormalities (congenital heart disease, valvar abnormalities) must be identified [127]. Most prospective donors are mechanically ventilated, which can lead to poor TTE imaging, particularly in older patients. Indeed, one study in adults showed technically inadequate TTE images in up to 29 % of mechanically ventilated brain-dead potential donors [128]. Thus when TTE assessment is inadequate, TEE evaluation must be performed.
- *Evaluation of ventricular assist device implantation*. The term ventricular assist device (VAD) refers to a broad range of mechanical circulatory devices designed to

Table 16.10 Doppler parameters across prosthetic aortic and mitral valves

Parameter	Normal	Possible stenosis	Suggests significant stenosis
Aortic mechanical, stented valves			
Peak velocity (m/s)	<3	3–4	>4
Mean gradient (mmHg)	<20	20–35	>35
DVI	≥0.30	0.29–0.25	<0.25
Effective Orifice Area (cm^2)	>1.2	1.2–0.8	<0.8
Contour of jet velocity through prosthetic aortic valve	Triangular, early peaking	Triangular to intermediate	Rounded, symmetrical contour
Acceleration time (ms)	<80	80–100	>00
Other pertinent findings: left ventricular size, function, hypertrophy			
Mitral valve prostheses			
Peak velocity (m/s)	<1.9	1.9	≥2.5
Mean gradient (mmHg)	≤5	6–10	>10
VTI (PrMV)/VTI (LVOT)	<2.2	2.2–25.	>2.5
Effective Orifice Area (cm^2)	≥2.0	1–2	<1
Pressure half-time (ms)	<130	130–200	>200
Other pertinent findings: left ventricular size and function, left atrial size, right ventricular size and function, estimation of pulmonary artery pressure			

From: Zoghbi et al [107]; with permission from Elsevier
DVI Doppler velocity index, equal to Velocity (Left ventricular outflow tract)/Velocity (Prosthetic aortic valve), *VTI* Velocity time integral, *PrMV* Prosthetic mitral valve, *LVOT* Left ventricular outflow tract

unload the failing heart, while at the same time provide adequate systemic (and in some cases pulmonary) perfusion [129]. These VADs are increasingly being utilized for patients with myocardial dysfunction, generally as a "bridge" to cardiac transplantation. Assist devices can be univentricular or biventricular, and there are two major types: pulsatile and continuous pumps. A number of VADs are currently available, and a full discussion of all these devices is beyond the scope of this chapter. Most of these devices are designed for the adult population; only a small number are available specifically for use in the pediatric population [130, 131], the most well-known being the Berlin Heart (EXCOR®), which will be the example used for the following discussion. The Berlin Heart is a paracorporeal pulsatile VAD that is connected to a pneumatically driven external pump to provide pulsatile flow into the aorta. For left sided assist, an inlet cannula is placed in the apex of the left ventricle (or rarely, the left atrium) (Fig. 16.27). Blood flows through this cannula to an extracorporeal pump. A pneumatic force from a separate driving unit is used to compress a membrane in the pump, expelling the blood into the systemic circulation through a separate arterial cannula connected to the ascending aorta, representing the device outflow [132]. The extracorporeal blood pump is available in a variety of volume sizes between 10–80 ml (Fig. 16.27), enabling use for the entire pediatric age range, including neonates [129] For right ventricular assist, a similar procedure is performed with the receiving cannula in the right atrium, and the arterial cannula in the pulmonary artery. A recent prospective multicenter study showed a clear survival advantage of the Berlin Heart (left or biventricular VAD) vs. extracorporeal membrane oxygenation as a bridge to heart transplantation [133].

For left sided VAD placement, intraoperative TEE serves several important roles. It is utilized to exclude important cardiac defects that could cause an intracardiac right to left shunt (e.g. patent foramen ovale) or compromise physiology after device placement (e.g. significant aortic regurgitation or mitral stenosis) [134]. In addition, TEE is used to evaluate the sites of device implantation within the heart, specifically the inflow connection to the atrium or ventricle, and the outflow connection to the aorta. Right and left ventricular size and function can also be assessed before and after device placement [135, 136]. Color flow and spectral Doppler are used to evaluate the flow characteristics into and out from the device. Thrombus in the cardiac chambers or attached to the inflow/outflow cannulae (if present) can also be evaluated. Monitoring for intracardiac air and appropriate de-airing also represent important applications of TEE in this setting. The type of cardiac connections, as well as the expected flow characteristics of a device, will vary by manufacturer, and these should be determined prior to performing the TEE [134]. An example of TEE evaluation of a Berlin Heart left sided VAD implantation is shown in Fig. 16.28, Video 16.21.

Following VAD implantation, echocardiography should be used for ongoing evaluation and monitoring while the patient is on support. Transthoracic echocar-

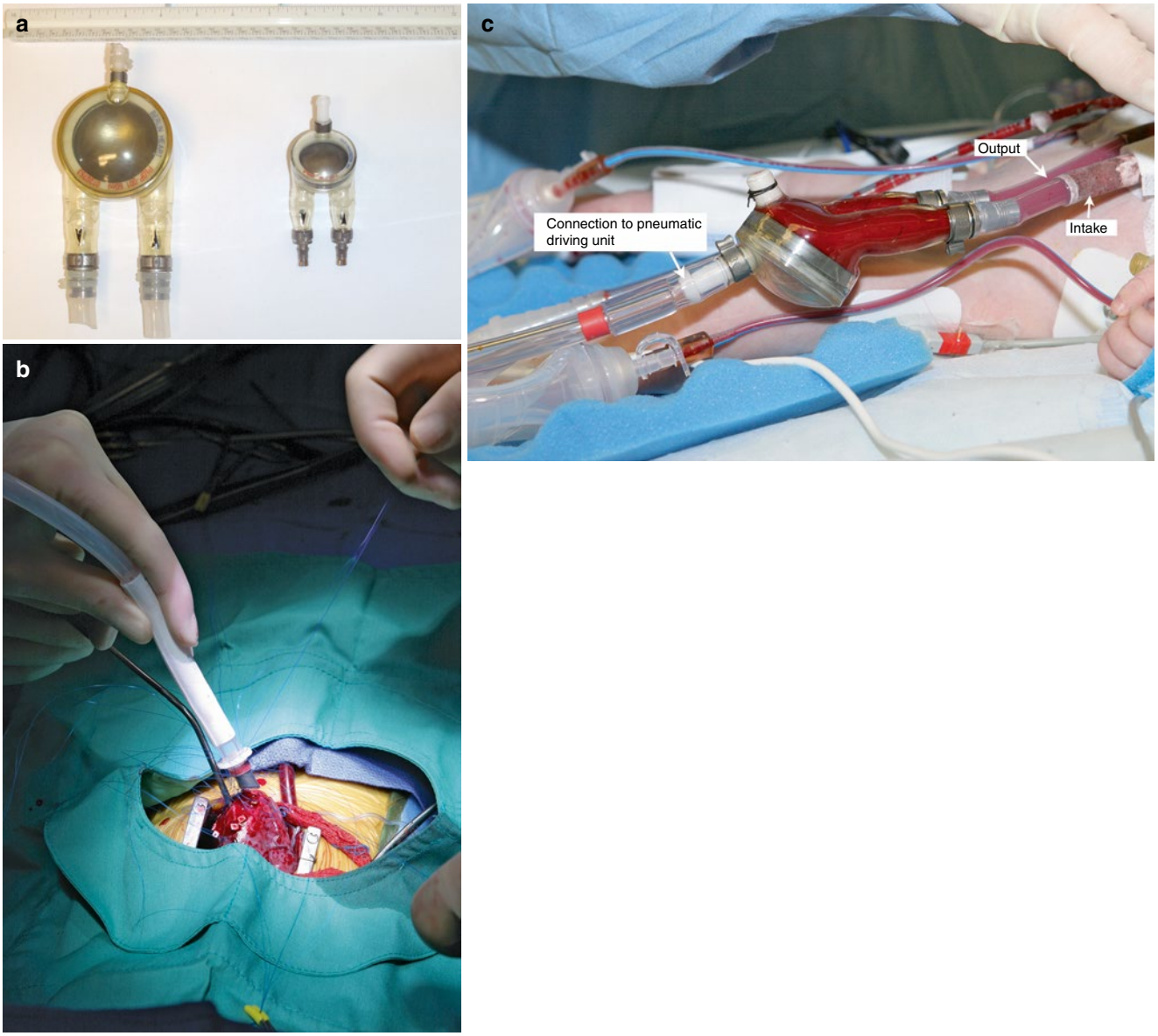

Fig. 16.27 Pictures of Berlin Heart. Figure **a** shows a pump for an older child (60 ml) on the *left*, next to an infant pump (10 ml) on the *right*. Figure **b** shows the intake cannula being implanted in the left ventricular apex. Figure **c** shows a pediatric pump that has been implanted. The intake and output cannulas enter the patient's thorax, as shown by the two tubes. The other tube is connected to the external pneumatic driving unit

diography generally suffices for these purposes, but TEE can also be used in selected patients in whom precordial echocardiographic windows are suboptimal or nonexistent. Ongoing evaluation should involve assessment of cannula position, and chamber size/function, as well as surveillance for possible valvular abnormalities, pericardial effusion/hematoma, intracardiac thrombus, endocarditis, and aortic dissection [137].

Note: The reader should be aware that an increasing number of new VAD designs are undergoing development for both adult and pediatric patients, so the variety of devices available for pediatric patients (pulsatile and continuous) is likely to widen considerably in the near future [138, 139]. The National Heart, Lung and Blood Institute (NHLBI) has been very active in this endeavor; in 2004 they initiated a 5 year program to develop a family of pediatric circulatory support devices [140]. Based on the results and progress made from this program, in 2010 the NHLBI created another support program—known as Pumps for Kids, Infants and Neonates (**PumpKIN**)—in which awards were granted to selected contractors (several of whom participated in the previous program) enabling them to begin the work necessary to receive Investigational Device Exemptions from the Food and Drug Administration for pediatric circulatory support devices. These devices will soon be ready for clinical trials [140, 141].

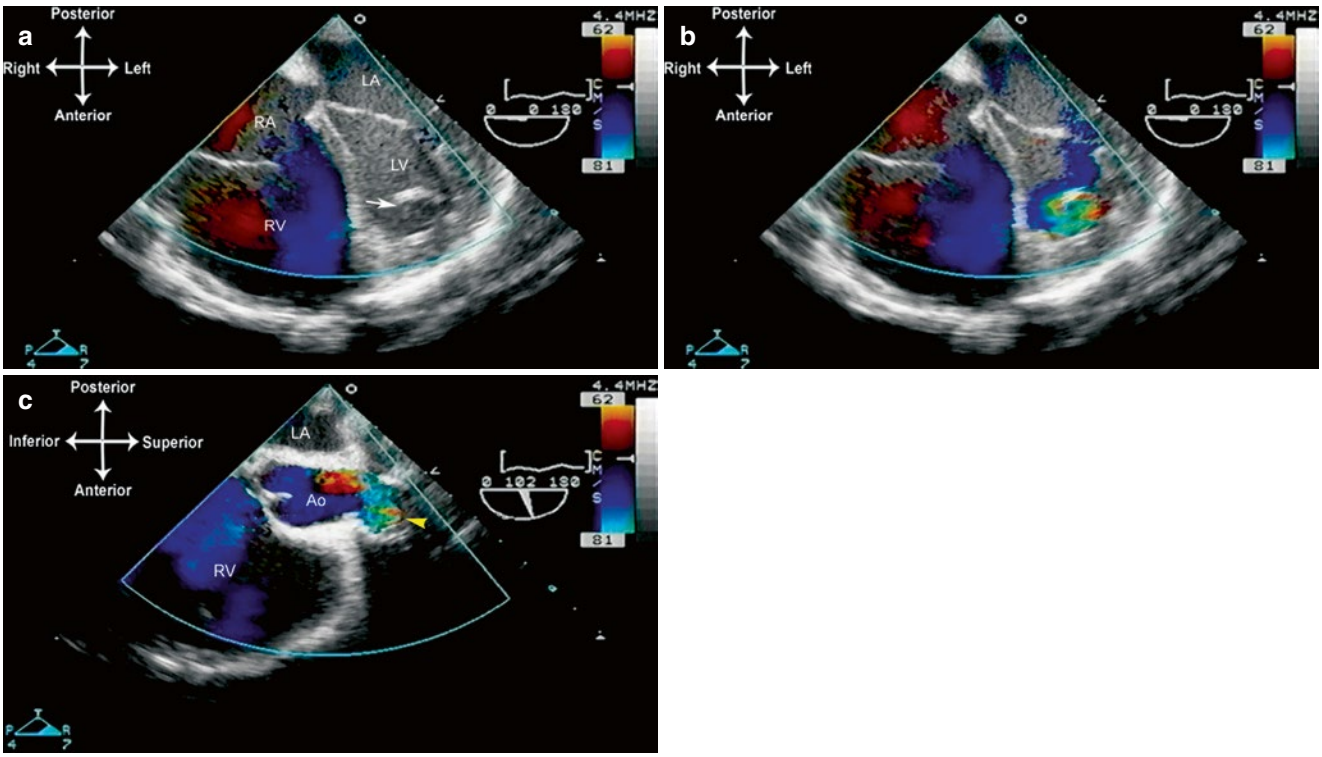

Fig. 16.28 Berlin Heart placement in a patient with dilated cardiomyopathy. Mid esophageal four chamber view, multiplane angle 0° (**a**, **b**) and 100° (**c**). The cannula (*arrow*) in the left ventricular apex withdraws blood returning from the left atrium. (**a**, **b**) When the blood has sufficiently filled the chamber in the device, it is pumped into the ascending aorta (*yellow arrowhead*), as shown from mid esophageal aortic valve long axis view, multiplane angle 102° (**c**). *Ao* aorta, *LA* left atrium, *LV* left ventricle, *RA* right atrium, *RV* right ventricle

- *Intraoperative monitoring/assessment of transplantation*. A preoperative TEE assessment during heart transplantation, if performed, is generally of limited utility. Since the recipient heart will be removed and replaced, most intracardiac anatomic and functional information regarding the recipient's native heart is irrelevant. However there could be some elements that have bearing upon the operative and postoperative course, particularly in patients with CHD. Specifically, abnormalities of cardiac position, systemic and pulmonary venous connections, and aortic/pulmonary artery anomalies (e.g. pulmonary atresia) need to be verified, as they could affect how an anatomically "normal" donor heart is implanted. Extra systemic venous or great artery length might need to be harvested for congenitally abnormal hearts. Additional useful information includes estimation of pulmonary arterial pressure (by tricuspid regurgitant jet velocity, if available).
- *Postoperative assessment of heart transplantation* requires an understanding of the current surgical technique, which enables the examiner to assess and recognize possible complications. Typically, the heart transplant procedure involves a systemic venous bicaval anastomosis (donor SVC/IVC to the recipient SVC/IVC), anastomosis of a recipient left atrial cuff to a cuff fashioned from the donor left atrium, and main pulmonary artery/aortic anastomoses between donor and recipient great arteries. The composite left atrial anastomosis gives the post-transplant left atrium a dilated and "hourglass" appearance with a prominent ridge that could be confused for thrombus [142] (Fig. 16.29, Video 16.22). The postoperative TEE assessment of heart transplantation is comprehensive, evaluating a number of different factors: any residual congenital cardiac defect (e.g. patent foramen ovale), possible retained intracardiac

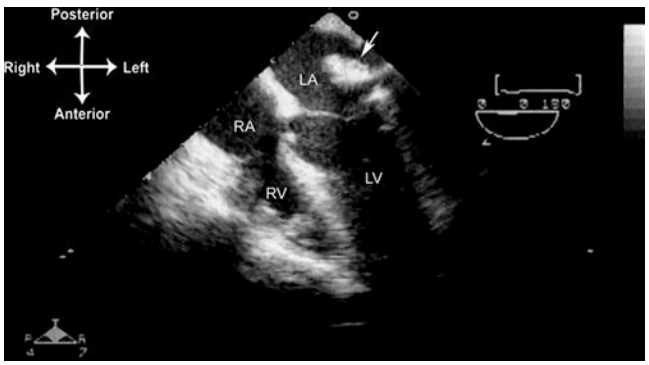

Fig. 16.29 Following heart transplantation, imaging in the mid esophageal four chamber view, multiplane angle 0°. The anastomosis of the donor left atrium to the cuff of the recipient left atrium creates an area of echogenicity (*arrow*) that can be mistaken for thrombus. *LA* left atrium, *LV* left ventricle, *RA* right atrium, *RV* right ventricle

air, intracardiac thrombus, right and left ventricular systolic function, AV and semilunar valve function, estimation of pulmonary artery pressure, and the patency of the donor-recipient anastomoses—aortic, pulmonary arterial, systemic and pulmonary veins [142, 143]. These assessments are particularly important when cardiac transplantation is performed in a patient with a complex form of CHD, e.g. dextrocardia or heterotaxy, and the possibility exists of kinking or torsion of these anastomoses [144]. Immediately following heart transplantation, overall biventricular systolic function is usually normal, although there can be paradoxical ventricular septal motion that can be expected to resolve with time. Also, right ventricular function can be affected if pulmonary vascular resistance is elevated [145].

- *Assessment of post-transplant cardiac allograft function in the intensive care unit*. Assessment of the transplanted heart essentially mirrors that of the postoperative TEE study discussed above. Other potential indications for TEE evaluation include surveillance for sources of systemic emboli, and also evaluation of possible pericardial effusion. Again, since TTE is usually sufficient, TEE is reserved for those patients with poor transthoracic acoustic images and/or when an open sternum prevents effective transthoracic imaging.

Evaluation of Lung Transplantation

In lung transplantation, cadaveric or living donor lungs are transplanted into a recipient with end-stage pulmonary or pulmonary vascular disease. For each lung (or lobe) transplanted, the donor mainstem (or lobar) bronchus, branch pulmonary artery, and pulmonary venous cuff are anastomosed to the corresponding structures in the recipient [146]. There are specific applications of TEE for lung transplant patients [147]. The preoperative TEE study is used to evaluate cardiac anatomy and exclude any potential intracardiac defects, e.g. small atrial septal defect, which should be addressed at the time of transplantation. Right and left heart function should also be assessed, because impaired cardiac function can have significant impact on the post-transplant outcome. The postoperative TEE study is used to assess the pulmonary arterial and venous anastomoses, as well as cardiac function and AV and semilunar valve function [148]. If tricuspid or pulmonary regurgitant jets are present, they can be used to estimate pulmonary arterial pressure. The evaluation of pulmonary venous return is one of the most important applications of TEE for post-lung transplant assessment. Because of its proximity to the left atrium and pulmonary veins, TEE provides superior imaging for pulmonary venous imaging and color flow/spectral Doppler evaluation (Chap. 4). Stenosis, kinking, or thrombosis of the pulmonary venous anastomosis—a very serious complication of lung transplantation—is readily detectable by TEE (Fig. 16.30, Video 16.23). In contrast, TTE imaging and color flow Doppler display of the pulmonary venous anastomoses is often inadequate, particularly in the immediate post-transplant period. Hence TEE evaluation should be strongly considered whenever there is a possibility of pulmonary venous obstruction in the lung transplant patient [149, 150].

Evaluation of Aortic Dissection

Aortic dissection is characterized by a separation in the ascending aortic wall between intima and media, resulting in a large intimal flap that separates a false from a true lumen in the ascending or descending aorta (or both). It is seen much more commonly in the adult age group (higher incidence of males than females, with a ratio between 2:1 to 5:1), with the most frequently associated condition being hypertension in approximately 80–90 % of patients [151, 152]. However, congenital abnormalities of aortic wall—notably Marfan syndrome, Loeys-Dietz syndrome, vascular Ehlers-Danlos, and other connective tissue abnormalities—are also associated with aortic dissection [153]. Recently, patients with Turner syndrome have also been reported to have an increased risk of aortic dilatation and aortic dissection [154]. Other congenital abnormalities that might predispose to an "aortopathy" and aortic dissection include bicuspid aortic valve, aortic coarctation, and iatrogenic causes such as cannula insertion or balloon dilation of coarctation [155]. The etiology is thought to be due to rupture of *vasa vasorum* but increased shear forces, and abnormalities of aortic media, can also result in intimal tears that ultimately lead to dissection. Left undiagnosed, aortic dissection can be a dangerous and potentially catastrophic condition, with complications including rupture, pericardial tamponade, aortic regurgitation, and coronary artery ischemia [152, 156].

Aortic dissection is commonly classified using either the Stanford or DeBakey classifications, both of which are based upon the location of the dissection. Stanford A involves the ascending aorta; Stanford B involves the descending aorta [157]. DeBakey I involves ascending and descending aorta, as well as the aortic arch; DeBakey II involves only the ascending aorta; DeBakey III involves only the descending aorta [158]. Typically, ascending aortic dissections (Stanford A, DeBakey II) carry much higher risk for complications compared to descending aortic dissections [152].

While other imaging modalities such as cardiac magnetic resonance imaging and computed tomography have assumed a primary role in the diagnosis of this condition, TEE provides an excellent imaging alternative, offering great sensitivity and specificity because of its superior spatial and temporal resolution [153, 159, 160]. Moreover, because of its portability and availability, TEE (when performed jointly with TTE imaging) is expeditious and can serve as rapid means to secure a diagnosis, particularly in an unstable patient. The advantage of TEE over static

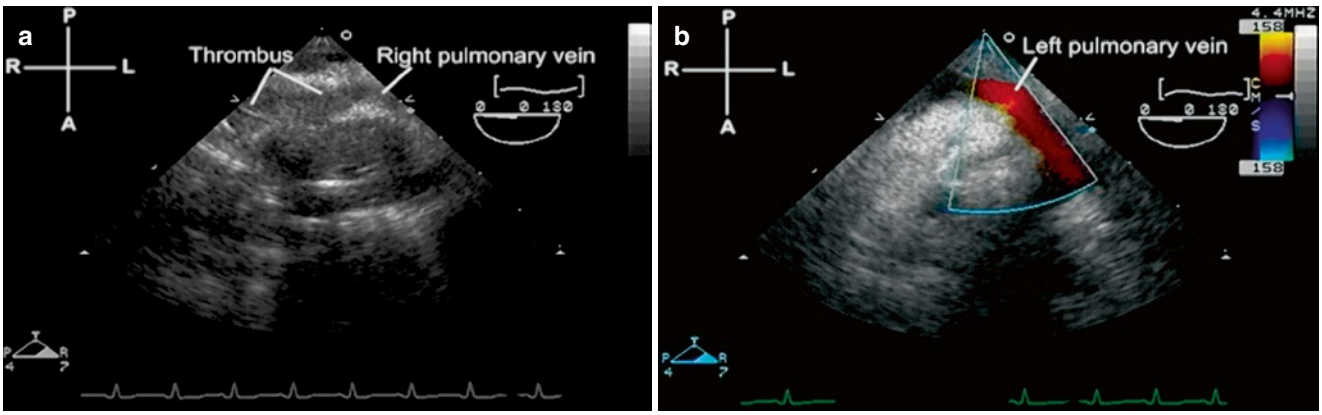

Fig. 16.30 Post-lung transplant, with thrombosis of the right pulmonary veins due to external compression by a large lymph node. Mid esophageal view, multiplane angle 0°. Figure **a** shows extensive thrombus in the right pulmonary veins. No flow was seen in the vessel by color flow Doppler. Figure **b** shows normal flow in the contralateral left pulmonary veins

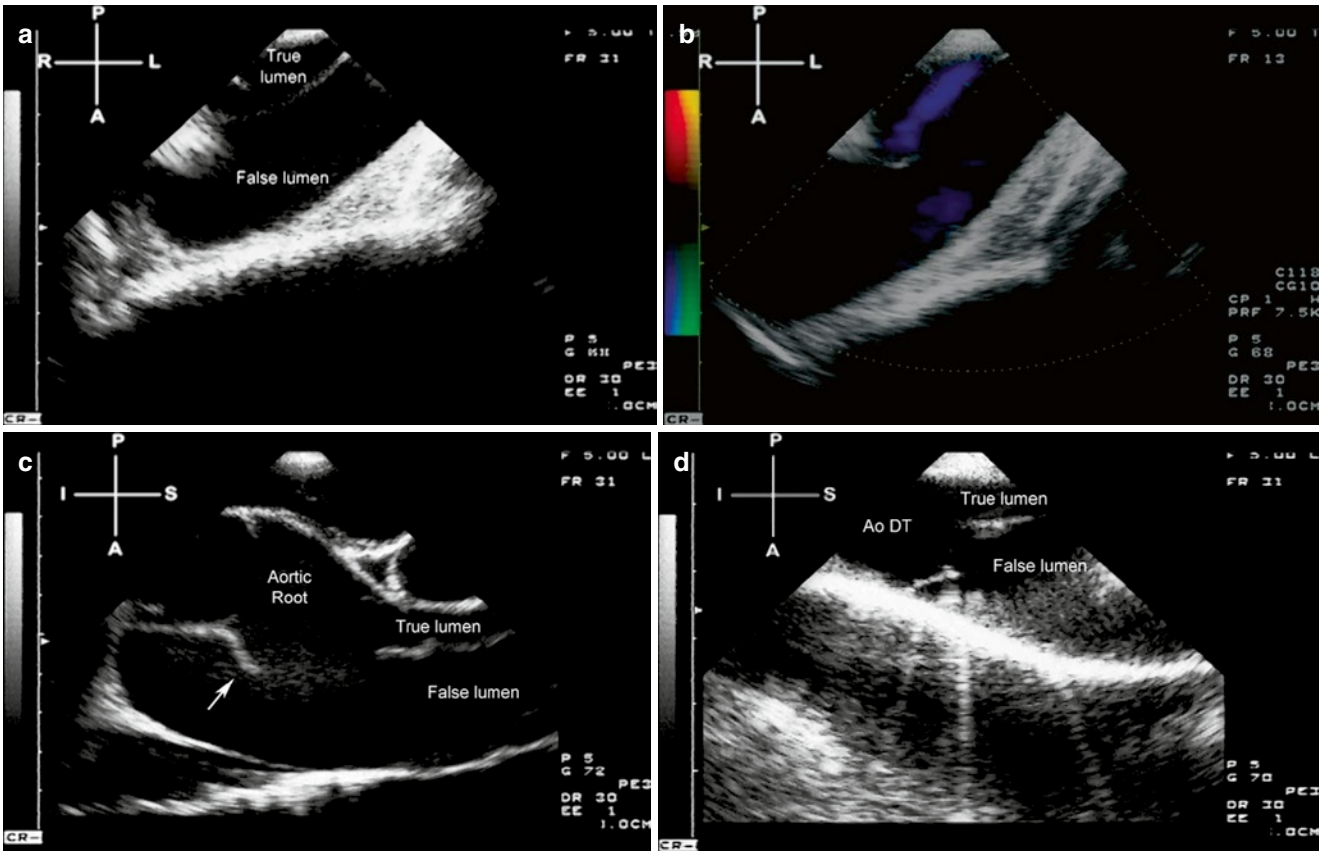

Fig. 16.31 Dissection of the ascending and descending aorta (DeBakey Type I) in a patient with Marfan syndrome. The patient also had a dilated aortic root and significant aortic valve regurgitation. (**a**) Upper esophageal aortic arch long axis view, multiplane angle 0°, shows true and false lumens. The false lumen is much larger than the true lumen in the ascending aorta and aortic arch. (**b**) Retrograde diastolic flow reversal is seen only in the true lumen by color flow mapping. (**c**) Mid esophageal aortic valve long axis view, multiplane angle 90°, shows the intimal flap (*arrow*) and true and false lumens. (**d**) Mid esophageal descending aortic long axis view, multiplane angle 90° (probe rotated leftward) shows the dissection extending into descending aorta. *AoDT* descending thoracic aorta

imaging modalities is that it readily detects and evaluates aortic regurgitation and pericardial effusion, and also assists in intraoperative assessment, although it cannot assess the abdominal aorta [161].

The aortic arch can be seen and evaluated by TEE, but the position of the esophagus in relation to the aortic arch presents some challenges. Unlike TTE, the entire aortic arch and descending aorta cannot be visualized in one plane, and

instead must be evaluated in sections with a combination of multiplane angles, and rotation of the TEE probe. At the same time, the probe must be alternately advanced and withdrawn to visualize the more superior and inferior portions of the entire aorta. Because of the possibility of artifacts mimicking a dissection, an important practice in two-dimensional echocardiography is to visualize the abnormality in more than one plane. Therefore, several multiplane angles (preferably orthogonal) should be utilized to confirm the intra-luminal presence of the flap, and color flow Doppler can be used to show the flow patterns in and out of the false lumen. For ascending aortic evaluation, the most important views include the mid to upper esophageal views—the mid esophageal ascending aortic short and long axis views (ME Asc Ao SAX, ME Asc Ao LAX), as well as the upper esophageal ascending aortic arc long and short axis views (UE Ao Arch LAX, UE Ao Arch SAX). With the upper esophageal views, slow probe rotation from right to left will display the ascending aorta, then aortic arch, and finally descending aorta. The probe can be alternately advanced and withdrawn to visualize various portions of these structures. The descending aorta is best visualized by rotation of the probe so that faces posteriorly and away from the heart, using the descending aorta short and long axis views (Desc Ao SAX, Desc Ao LAX) to achieve orthogonal tomographic images, while withdrawing/advancing the probe to evaluate the different portions of the descending thoracic aorta [152].

Whether the dissection affects the ascending or descending aorta (or both), the characteristic echocardiographic feature of the dissection remains the same: intimal disruption that manifests as a thin, mobile intimal flap, separating the aorta into true and false lumens. In many instances, the false lumen is larger than the true lumen. There can be one or more re-entry sites between true and false lumens. Color flow Doppler will often show a difference in flow patterns between the true and false lumens; there can be much lower Doppler flow velocity in the false lumen, and spontaneous echo contrast or thrombus formation will sometimes be present [152]. In some cases, flow in the two lumens occurs in opposite directions, e.g. when aortic regurgitation is present (Fig. 16.31, Video 16.24). Because disruption of the aortic valve, aortic root, sinuses and coronary artery ostia may be associated with an aortic dissection, it is important to assess valve competence and global as well as segmental ventricular systolic function during the TEE evaluation.

Summary

This chapter reviewed a number of additional areas in which TEE has applications for the pediatric and young adult population. Some of these applications pertain equally to patients with and without congenital heart disease, and some have significant overlap with TEE as it is performed in adult patients with cardiac disease. These additional applications illustrate the wide applicability and important additive value that TEE can provide in cardiac patients of all ages.

References

1. Karchmer AW. Infective endocarditis. In: Bonow RO, Mann DL, Zipes DP, Libby P, editors. Braunwald's heart disease: a textbook of cardiovascular medicine. 9th ed. Philadelphia: Elsevier Saunders; 2012. p. 1540–60.
2. McDonald JR. Acute infective endocarditis. Infect Dis Clin North Am. 2009;23:643–64.
3. Bayer AS, Bolger AF, Taubert KA, et al. Diagnosis and management of infective endocarditis and its complications. Circulation. 1998;98:2936–48.
4. Ferrieri P, Gewitz MH, Gerber MA, et al. Unique features of infective endocarditis in childhood. Circulation. 2002;105:2115–26.
5. Saiman L, Prince A, Gersony WM. Pediatric infective endocarditis in the modern era. J Pediatr. 1993;122:847–53.
6. Morris CD, Reller MD, Menashe VD. Thirty-year incidence of infective endocarditis after surgery for congenital heart defect. JAMA. 1998;279:599–603.
7. Lin YT, Hsieh KS, Chen YS, Huang IF, Cheng MF. Infective endocarditis in children without underlying heart disease. J Microbiol Immunol Infect. 2012;46:121–8.
8. Durack DT, Lukes AS, Bright DK. New criteria for diagnosis of infective endocarditis: utilization of specific echocardiographic findings. Duke Endocarditis Service. Am J Med. 1994;96:200–9.
9. Li JS, Sexton DJ, Mick N, et al. Proposed modifications to the Duke criteria for the diagnosis of infective endocarditis. Clin Infect Dis. 2000;30:633–8.
10. Baddour LM, Wilson WR, Bayer AS, et al. Infective endocarditis: diagnosis, antimicrobial therapy, and management of complications: a statement for healthcare professionals from the Committee on Rheumatic Fever, Endocarditis, and Kawasaki Disease, Council on Cardiovascular Disease in the Young, and the Councils on Clinical Cardiology, Stroke, and Cardiovascular Surgery and Anesthesia, American Heart Association: endorsed by the Infectious Diseases Society of America. Circulation. 2005;111:e394–434.
11. Bayer AS, Ward JI, Ginzton LE, Shapiro SM. Evaluation of new clinical criteria for the diagnosis of infective endocarditis. Am J Med. 1994;96:211–9.
12. Del Pont JM, De Cicco LT, Vartalitis C, et al. Infective endocarditis in children: clinical analyses and evaluation of two diagnostic criteria. Pediatr Infect Dis J. 1995;14:1079–86.
13. Hoen B, Beguinot I, Rabaud C, et al. The Duke criteria for diagnosing infective endocarditis are specific: analysis of 100 patients with acute fever or fever of unknown origin. Clin Infect Dis. 1996;23:298–302.
14. Stockheim JA, Chadwick EG, Kessler S, et al. Are the Duke criteria superior to the Beth Israel criteria for the diagnosis of infective endocarditis in children? Clin Infect Dis. 1998;27:1451–6.
15. Tissieres P, Gervaix A, Beghetti M, Jaeggi ET. Value and limitations of the von Reyn, Duke, and modified Duke criteria for the diagnosis of infective endocarditis in children. Pediatrics. 2003;112:e467.
16. Prendergast BD. Diagnostic criteria and problems in infective endocarditis. Heart. 2004;90:611–3.
17. Bonow RO, Carabello BA, Chatterjee K, et al. 2008 Focused update incorporated into the ACC/AHA 2006 guidelines for the management of patients with valvular heart disease: a report of

the American College of Cardiology/American Heart Association Task Force on Practice Guidelines (Writing Committee to Revise the 1998 Guidelines for the Management of Patients With Valvular Heart Disease): endorsed by the Society of Cardiovascular Anesthesiologists, Society for Cardiovascular Angiography and Interventions, and Society of Thoracic Surgeons. Circulation. 2008;118:e523–661.
18. Tornos P, Iung B, Permanyer-Miralda G, et al. Infective endocarditis in Europe: lessons from the Euro heart survey. Heart. 2005;91:571–5.
19. Prendergast BD, Tornos P. Surgery for infective endocarditis: who and when? Circulation. 2010;121:1141–52.
20. Kang D-H, Kim Y-J, Kim S-H, et al. Early surgery versus conventional treatment for infective endocarditis. N Engl J Med. 2012;366: 2466–73.
21. Alexiou C, Langley SM, Monro JL. Surgery for infective valve endocarditis in children. Eur J Cardiothorac Surg. 1999;16: 653–9.
22. Karaci AR, Aydemir NA, Harmandar B, et al. Surgical treatment of infective valve endocarditis in children with congenital heart disease. J Card Surg. 2012;27:93–8.
23. Nomura F, Penny DJ, Menahem S, Pawade A, Karl TR. Surgical intervention for infective endocarditis in infancy and childhood. Ann Thorac Surg. 1995;60:90–5.
24. Martin JM, Neches WH, Wald ER. Infective endocarditis: 35 years of experience at a children's hospital. Clin Infect Dis. 1997;24:669–75.
25. Knirsch W, Nadal D. Infective endocarditis in congenital heart disease. Eur J Pediatr. 2011;170:1111–27.
26. Durack DT, Beeson PB. Experimental bacterial endocarditis. I. Colonization of a sterile vegetation. Br J Exp Pathol. 1972;53:44–9.
27. Fernicola DJ, Roberts WC. Frequency of ring abscess and cuspal infection in active infective endocarditis involving biologic valves. Am J Cardiol. 1993;72:314–23.
28. Daniel WG, Mugge A, Martin RP, et al. Improvement in the diagnosis of abscesses associated with endocarditis by transesophageal echocardiography. N Engl J Med. 1991;324:795–800.
29. Shaffer EM, Snider AR, Beekman RH, Behrendt DM, Peschiera AW. Sinus of Valsalva aneurysm complicating bacterial endocarditis in an infant: diagnosis with two-dimensional and Doppler echocardiography. J Am Coll Cardiol. 1987;9:588–91.
30. Anguera I, Miro JM, Vilacosta I, et al. Aorto-cavitary fistulous tract formation in infective endocarditis: clinical and echocardiographic features of 76 cases and risk factors for mortality. Eur Heart J. 2005;26:288–97.
31. Kearney RA, Eisen HJ, Wolf JE. Nonvalvular infections of the cardiovascular system. Ann Intern Med. 1994;121:219–30.
32. Sievers H-H, Stierle U, Charitos EI, et al. Major adverse cardiac and cerebrovascular events after the Ross procedure: a report from the German-Dutch Ross Registry. Circulation. 2010;122: S216–23.
33. Mills J, Utley J, Abbott J. Heart failure in infective endocarditis: predisposing factors, course, and treatment. Chest. 1974;66:151–7.
34. Pelletier LLJ, Petersdorf RG. Infective endocarditis: a review of 125 cases from the University of Washington Hospitals, 1963–72. Medicine (Baltimore). 1977;56:287–313.
35. Hasbun R, Vikram HR, Barakat LA, Buenconsejo J, Quagliarello VJ. Complicated left-sided native valve endocarditis in adults: risk classification for mortality. JAMA. 2003;289:1933–40.
36. Ryan EW, Bolger AF. Transesophageal echocardiography (TEE) in the evaluation of infective endocarditis. In: Foster E, editor. Cardiology clinics: transesophageal echocardiography. San Francisco; Division of Cardiology, Department of Medicine, University of California; 2000. p. 773–87.
37. Erbel R, Rohmann S, Drexler M, et al. Improved diagnostic value of echocardiography in patients with infective endocarditis by transoesophageal approach. A prospective study. Eur Heart J. 1988;9:43–53.
38. Shanewise JS, Martin RP. Assessment of endocarditis and associated complications with transesophageal echocardiography. Crit Care Clin. 1996;12:411–27.
39. Jacob S, Tong AT. Role of echocardiography in the diagnosis and management of infective endocarditis. Curr Opin Cardiol. 2002;17:478–85.
40. Reynolds HR, Jagen MA, Tunick PA, Kronzon I. Sensitivity of transthoracic versus transesophageal echocardiography for the detection of native valve vegetations in the modern era. J Am Soc Echocardiogr. 2003;16:67–70.
41. Daniel WG, Mugge A, Grote J, et al. Comparison of transthoracic and transesophageal echocardiography for detection of abnormalities of prosthetic and biologic valves in the mitral and aortic positions. Am J Cardiol. 1993;71:210–5.
42. Penk JS, Webb CL, Shulman ST, Anderson EJ. Echocardiography in pediatric infective endocarditis. Pediatr Infect Dis J. 2011;30: 1109–11.
43. Humpl T, McCrindle BW, Smallhorn JF. The relative roles of transthoracic compared with transesophageal echocardiography in children with suspected infective endocarditis. J Am Coll Cardiol. 2003;41:2068–71.
44. Steckelberg JM, Murphy JG, Ballard D, et al. Emboli in infective endocarditis: the prognostic value of echocardiography. Ann Intern Med. 1991;114:635–40.
45. Lopez JA, Ross RS, Fishbein MC, Siegel RJ. Nonbacterial thrombotic endocarditis: a review. Am Heart J. 1987;113:773–84.
46. Asopa S, Patel A, Khan OA, Sharma R, Ohri SK. Non-bacterial thrombotic endocarditis. Eur J Cardiothorac Surg. 2007;32:696–701.
47. González Quintela A, Candela MJ, Vidal C, Román J, Aramburo P. Non-bacterial thrombotic endocarditis in cancer patients. Acta Cardiol. 1991;46:1–9.
48. Beynon RP, Bahl VK, Prendergast BD. Infective endocarditis. BMJ. 2006;333:334–9.
49. Asinger RW, Dyken ML, Fisher M, Hart RG, Sherman DG. Cardiogenic brain embolism. The second report of the Cerebral Embolism Task Force. Arch Neurol. 1989;46:727–43.
50. Agmon Y, Khandheria BK, Gentile F, Seward JB. Echocardiographic assessment of the left atrial appendage. J Am Coll Cardiol. 1999;34: 1867–77.
51. de Divitiis M, Omran H, Rabahieh R, et al. Right atrial appendage thrombosis in atrial fibrillation: its frequency and its clinical predictors. Am J Cardiol. 1999;84:1023–8.
52. Ozer O, Sari I, Davutoglu V. Right atrial appendage: forgotten part of the heart in atrial fibrillation. Clin Appl Thromb Hemost. 2010;16:218–20.
53. Schweizer P, Bardos P, Erbel R, et al. Detection of left atrial thrombi by echocardiography. Br Heart J. 1981;45:148–56.
54. Aschenberg W, Schluter M, Kremer P, Schroder E, Siglow V, Bleifeld W. Transesophageal two-dimensional echocardiography for the detection of left atrial appendage thrombus. J Am Coll Cardiol. 1986;7:163–6.
55. Manning WJ, Weintraub RM, Waksmonski CA, et al. Accuracy of transesophageal echocardiography for identifying left atrial thrombi. A prospective, intraoperative study. Ann Intern Med. 1995;123:817–22.
56. Veinot JP, Harrity PJ, Gentile F, et al. Anatomy of the normal left atrial appendage: a quantitative study of age-related changes in 500 autopsy hearts: implications for echocardiographic examination. Circulation. 1997;96:3112–5.
57. Karakus G, Kodali V, Inamdar V, Nanda NC, Suwanjutah T, Pothineni KR. Comparative assessment of left atrial appendage by transesophageal and combined two- and three-dimensional transthoracic echocardiography. Echocardiography. 2008;25: 918–24.

58. Werner JA, Cheitlin MD, Gross BW, Speck SM, Ivey TD. Echocardiographic appearance of the Chiari network: differentiation from right-heart pathology. Circulation. 1981;63:1104–9.
59. Black IW. Spontaneous echo contrast: where there's smoke there's fire. Echocardiography. 2000;17:373–82.
60. Kwaan HC, Sakurai S, Wang J. Rheological abnormalities and thromboembolic complications in heart disease: spontaneous echo contrast and red cell aggregation. Semin Thromb Hemost. 2003;29: 529–34.
61. Chan HS, Sonley MJ, Moes CA, Daneman A, Smith CR, Martin DJ. Primary and secondary tumors of childhood involving the heart, pericardium, and great vessels. A report of 75 cases and review of the literature. Cancer. 1985;56:825–36.
62. Roberts WC. Primary and secondary neoplasms of the heart. Am J Cardiol. 1997;80:671–82.
63. Shapiro LM. Cardiac tumours: diagnosis and management. Heart. 2001;85:218–22.
64. Miyake CY, Del Nido PJ, Alexander ME, et al. Cardiac tumors and associated arrhythmias in pediatric patients, with observations on surgical therapy for ventricular tachycardia. J Am Coll Cardiol. 2011;58:1903–9.
65. Luck SR, DeLeon S, Shkolnik A, Morgan E, Labotka R. Intracardiac Wilms' tumor: diagnosis and management. J Pediatr Surg. 1982;17: 551–4.
66. Marx GR, Moran AM. Cardiac tumors. In: Allen HD, Dricoll DJ, Shaddy RE, Feltes TF, editors. Moss and Adams' heart disease in infants, children, and adolescents: including the fetus and young adult. 7th ed. Philadelphia: Lippincott Williams & Wilkins; 2008. p. 1479–95.
67. Uzun O, Wilson DG, Vujanic GM, Parsons JM, De Giovanni JV. Cardiac tumours in children. Orphanet J Rare Dis. 2007;2:11.
68. Günther T, Schreiber C, Noebauer C, Eicken A, Lange R. Treatment strategies for pediatric patients with primary cardiac and pericardial tumors: a 30-year review. Pediatr Cardiol. 2008;29:1071–6.
69. Becker AE. Primary heart tumors in the pediatric age group: a review of salient pathologic features relevant for clinicians. Pediatr Cardiol. 2000;21:317–23.
70. Burke AP, Rosado-de-Christenson M, Templeton PA, Virmani R. Cardiac fibroma: clinicopathologic correlates and surgical treatment. J Thorac Cardiovasc Surg. 1994;108:862–70.
71. Reynen K. Cardiac myxomas. N Engl J Med. 1995;333:1610–7.
72. Bulkley BH, Hutchins GM. Atrial myxomas: a fifty year review. Am Heart J. 1979;97:639–43.
73. Hada Y, Wolfe C, Murray GF, Craige E. Right ventricular myxoma. Case report and review of phonocardiographic and auscultatory manifestations. Am Heart J. 1980;100:871–7.
74. Leonhardt ET, Kullenberg KP. Bilateral atrial myxomas with multiple arterial aneurysms—a syndrome mimicking polyarteritis nodosa. Am J Med. 1977;62:792–4.
75. Perez de Isla L, de Castro R, Zamorano JL, et al. Diagnosis and treatment of cardiac myxomas by transesophageal echocardiography. Am J Cardiol. 2002;90:1419–21.
76. Burke A, Johns JP, Virmani R. Hemangiomas of the heart. A clinicopathologic study of ten cases. Am J Cardiovasc Pathol. 1990;3:283–90.
77. Niwa K, Tashima K, Terai M, Okajima Y, Nakajima H. Contrast-enhanced magnetic resonance imaging of cardiac tumors in children. Am Heart J. 1989;118:424–5.
78. Link KM, Lesko NM. MR evaluation of cardiac/juxtacardiac masses. Top Magn Reson Imaging. 1995;7:232–45.
79. Bardo DME. Cardiac magnetic resonance imaging signal characteristics of cardiac tumors in children. J Am Coll Cardiol. 2011;58: 1055–6.
80. Obeid AI, Marvasti M, Parker F, Rosenberg J. Comparison of transthoracic and transesophageal echocardiography in diagnosis of left atrial myxoma. Am J Cardiol. 1989;63:1006–8.
81. Geibel A, Kasper W, Keck A, Hofmann T, Konstantinides S, Just H. Diagnosis, localization and evaluation of malignancy of heart and mediastinal tumors by conventional and transesophageal echocardiography. Acta Cardiol. 1996;51:395–408.
82. Engberding R, Daniel WG, Erbel R, et al. Diagnosis of heart tumours by transoesophageal echocardiography: a multicentre study in 154 Patients. European Cooperative Study Group. Eur Heart J. 1993;14:1223–8.
83. Borges AC, Witt C, Bartel T, Muller S, Konertz W, Baumann G. Preoperative two- and three-dimensional transesophageal echocardiographic assessment of heart tumors. Ann Thorac Surg. 1996;61:1163–7.
84. Brown AS, Why H, Monaghan MJ. Value of multiplane transoesophageal echocardiography in recurrent atrial myxoma. Br Heart J. 1994;71:540.
85. Goldman JH, Foster E. Transesophageal echocardiographic (TEE) evaluation of intracardiac and pericardial masses. Cardiol Clin. 2000;18:849–60.
86. Ross DN. Replacement of aortic and mitral valves with a pulmonary autograft. Lancet. 1967;2:956–8.
87. Chambers JC, Somerville J, Stone S, Ross DN. Pulmonary autograft procedure for aortic valve disease: long-term results of the pioneer series. Circulation. 1997;96:2206–14.
88. Athanasiou T, Cherian A, Ross D. The Ross II procedure: pulmonary autograft in the mitral position. Ann Thorac Surg. 2004;78: 1489–95.
89. Protopapas AD, Athanasiou T. Contegra conduit for reconstruction of the right ventricular outflow tract: a review of published early and mid-time results. J Cardiothorac Surg. 2008;3:62.
90. Hickey EJ, McCrindle BW, Blackstone EH, et al. Jugular venous valved conduit (Contegra) matches allograft performance in infant truncus arteriosus repair. Eur J Cardiothorac Surg. 2008;33: 890–8.
91. Christenson JT, Sierra J, Colina Manzano NE, Jolou J, Beghetti M, Kalangos A. Homografts and xenografts for right ventricular outflow tract reconstruction: long-term results. Ann Thorac Surg. 2010;90:1287–93.
92. Dave H, Mueggler O, Comber M, et al. Risk factor analysis of 170 single-institutional contegra implantations in pulmonary position. Ann Thorac Surg. 2011;91:195–302; discussion 202–3.
93. Hopkins RA, editor. Tissue and bio-engineering for congenital cardiac disease. Prog Pediatr Cardiol. 2006;21(2):137–244.
94. Aslam AK, Aslam AF, Vasavada BC, Khan IA. Prosthetic heart valves: types and echocardiographic evaluation. Int J Cardiol. 2007;122:99–110.
95. Pibarot P, Dumesnil JG. Prosthetic heart valves: selection of the optimal prosthesis and long-term management. Circulation. 2009;119:1034–48.
96. Oosterhof T, Hazekamp MG, Mulder BJ. Opportunities in pulmonary valve replacement. Expert Rev Cardiovasc Ther. 2009;7:1117–22.
97. Kidane AG, Burriesci G, Cornejo P, et al. Current developments and future prospects for heart valve replacement therapy. J Biomed Mater Res B Appl Biomater. 2009;88:290–303.
98. Waterbolk TW, Hoendermis ES, den Hamer IJ, Ebels T. Pulmonary valve replacement with a mechanical prosthesis. Promising results of 28 procedures in patients with congenital heart disease. Eur J Cardiothorac Surg. 2006;30:28–32.
99. Fleming GA, Hill KD, Green AS, Rhodes JF. Percutaneous pulmonary valve replacement. Prog Pediatr Cardiol. 2012;33:143–50.
100. Momenah TS, El Oakley R, Al Najashi K, Khoshhal S, Al Qethamy H, Bonhoeffer P. Extended application of percutaneous pulmonary valve implantation. J Am Coll Cardiol. 2009;53:1859–63.
101. Hasan BS, McElhinney DB, Brown DW, et al. Short-term performance of the transcatheter Melody valve in high-pressure

hemodynamic environments in the pulmonary and systemic circulations. Circ Cardiovasc Interv. 2011;4:615–20.
102. Gurvitch R, Cheung A, Ye J, et al. Transcatheter valve-in-valve implantation for failed surgical biologic valves. J Am Coll Cardiol. 2011;58:2196–209.
103. Gillespie MJ, Dori Y, Harris MA, Sathanandam S, Glatz AC, Rome JJ. Bilateral branch pulmonary artery melody valve implantation for treatment of complex right ventricular outflow tract dysfunction in a high-risk patient. Circ Cardiovasc Interv. 2011; 4:e21–3.
104. Billings FT, Kodali SK, Shanewise JS. Transcatheter aortic valve implantation: anesthetic considerations. Anesth Analg. 2009;108:1453–62.
105. Kenny D, Hijazi ZM, Kar S, et al. Percutaneous implantation of the Edwards SAPIEN transcatheter heart valve for conduit failure in the pulmonary position: early phase 1 results from an international multicenter clinical trial. J Am Coll Cardiol. 2011;58:2248–56.
106. Webb JG, Wood DA. Current status of transcatheter aortic valve replacement. J Am Coll Cardiol. 2012;60:483–92.
107. Zoghbi WA, Chambers JB, Dumesnil JG, et al. Recommendations for evaluation of prosthetic valves with echocardiography and doppler ultrasound: a report From the American Society of Echocardiography's Guidelines and Standards Committee and the Task Force on Prosthetic Valves, developed in conjunction with the American College of Cardiology Cardiovascular Imaging Committee, Cardiac Imaging Committee of the American Heart Association, the European Association of Echocardiography, a registered branch of the European Society of Cardiology, the Japanese Society of Echocardiography and the Canadian Society of Echocardiography, endorsed by the American College of Cardiology Foundation, American Heart Association, European Association of Echocardiography, a registered branch of the European Society of Cardiology, the Japanese Society of Echocardiography, and Canadian Society of Echocardiography. J Am Soc Echocardiogr. 2009;22:975–1014.
108. Rosenhek R, Binder T, Maurer G, Baumgartner H. Normal values for Doppler echocardiographic assessment of heart valve prostheses. J Am Soc Echocardiogr. 2003;16:1116–27.
109. Bach DS. Transesophageal echocardiographic (TEE) evaluation of prosthetic valves. Cardiol Clin. 2000;18:751–71.
110. Morguet AJ, Werner GS, Andreas S, Kreuzer H. Diagnostic value of transesophageal compared with transthoracic echocardiography in suspected prosthetic valve endocarditis. Herz. 1995;20:390–8.
111. Schulz R, Werner GS, Fuchs JB, et al. Clinical outcome and echocardiographic findings of native and prosthetic valve endocarditis in the 1990's. Eur Heart J. 1996;17:281–8.
112. Lengyel M. The impact of transesophageal echocardiography on the management of prosthetic valve endocarditis: experience of 31 cases and review of the literature. J Heart Valve Dis. 1997;6:204–11.
113. Zoghbi WA, Enriquez-Sarano M, Foster E, et al. Recommendations for evaluation of the severity of native valvular regurgitation with two-dimensional and Doppler echocardiography. J Am Soc Echocardiogr. 2003;16:777–802.
114. Quiñones M. Echocardiographic assessment of valve stenosis: EAE/ASE recommendations for clinical practice. J Am Soc Echocardiogr. 2009;22:1–23.
115. Rahimtoola SH. The problem of valve prosthesis-patient mismatch. Circulation. 1978;58:20–4.
116. Pibarot P, Dumesnil JG. Hemodynamic and clinical impact of prosthesis-patient mismatch in the aortic valve position and its prevention. J Am Coll Cardiol. 2000;36:1131–41.
117. Mohty D, Mohty-Echahidi D, Malouf JF, et al. Impact of prosthesis-patient mismatch on long-term survival in patients with small St Jude Medical mechanical prostheses in the aortic position. Circulation. 2006;113:420–6.
118. Walther T, Rastan A, Falk V, et al. Patient prosthesis mismatch affects short- and long-term outcomes after aortic valve replacement. Eur J Cardiothorac Surg. 2006;30:15–9.
119. Rahimtoola SH. Choice of prosthetic heart valve in adults an update. J Am Coll Cardiol. 2010;55:2413–26.
120. Lam B-K, Chan V, Hendry P, et al. The impact of patient-prosthesis mismatch on late outcomes after mitral valve replacement. J Thorac Cardiovasc Surg. 2007;133:1464–73.
121. Blackstone EH, Cosgrove DM, Jamieson WR, et al. Prosthesis size and long-term survival after aortic valve replacement. J Thorac Cardiovasc Surg. 2003;126:783–96.
122. Koch CG, Khandwala F, Estafanous FG, Loop FD, Blackstone EH. Impact of prosthesis-patient size on functional recovery after aortic valve replacement. Circulation. 2005;111:3221–9.
123. Pibarot P, Dumesnil JG. Prosthesis-patient mismatch: definition, clinical impact, and prevention. Heart. 2006;92:1022–9.
124. Masuda M, Kado H, Tatewaki H, Shiokawa Y, Yasui H. Late results after mitral valve replacement with bileaflet mechanical prosthesis in children: evaluation of prosthesis-patient mismatch. Ann Thorac Surg. 2004;77:913–7.
125. Zamorano JL, Badano LP, Bruce C, et al. EAE/ASE recommendations for the use of echocardiography in new transcatheter interventions for valvular heart disease. J Am Soc Echocardiogr. 2011;24:937–65.
126. Holmes DR, Mack MJ, Kaul S, et al. 2012 ACCF/AATS/SCAI/STS expert consensus document on transcatheter aortic valve replacement. J Am Coll Cardiol. 2012;59:1200–54.
127. Zaroff J. Echocardiographic evaluation of the potential cardiac donor. J Heart Lung Transplant. 2004;23:S250–2.
128. Stoddard MF, Longaker RA. The role of transesophageal echocardiography in cardiac donor screening. Am Heart J. 1993;125:1676–81.
129. Hetzer R, Potapov EV, Alexi-Meskishvili V, et al. Single-center experience with treatment of cardiogenic shock in children by pediatric ventricular assist devices. J Thorac Cardiovasc Surg. 2011;141:616–23, 623.e1.
130. Cooper DS, Jacobs JP, Moore L, et al. Cardiac extracorporeal life support: state of the art in 2007. Cardiol Young. 2007;17 Suppl 2:104–15.
131. Potapov EV, Stiller B, Hetzer R. Ventricular assist devices in children: current achievements and future perspectives. Pediatr Transplant. 2007;11:241–55.
132. Hetzer R, Potapov EV, Stiller B, et al. Improvement in survival after mechanical circulatory support with pneumatic pulsatile ventricular assist devices in pediatric patients. Ann Thorac Surg. 2006;82:917–24; discussion 924–5.
133. Fraser CD, Jaquiss RDB, Rosenthal DN, et al. Prospective trial of a pediatric ventricular assist device. N Engl J Med. 2012; 367:532–41.
134. Chumnanvej S, Wood MJ, MacGillivray TE, Melo MFV. Perioperative echocardiographic examination for ventricular assist device implantation. Anesth Analg. 2007;105:583–601.
135. Davila-Roman VG, Barzilai B. Transesophageal echocardiographic evaluation of patients receiving mechanical assistance from ventricular assist devices. Echocardiography. 1997;14:505–12.
136. Scohy TV, Gommers D, Maat APWM, Dejong PL, Bogers AJJC, Hofland J. Intraoperative transesophageal echocardiography is beneficial for hemodynamic stabilization during left ventricular assist device implantation in children. Paediatr Anaesth. 2009; 19:390–5.
137. Sachdeva R, Frazier EA, Jaquiss RDB, Imamura M, Swearingen CJ, Vyas HV. Echocardiographic evaluation of ventricular assist devices in pediatric patients. J Am Soc Echocardiogr. 2013;26:41–9.

138. Baldwin JT, Duncan BW. Ventricular assist devices for children. Prog Pediatr Cardiol. 2006;21:173–84.
139. Miera O, Potapov EV, Redlin M, et al. First experiences with the HeartWare ventricular assist system in children. Ann Thorac Surg. 2011;91:1256–60.
140. Baldwin JT, Borovetz HS, Duncan BW, Gartner MJ, Jarvik RK, Weiss WJ. The national heart, lung, and blood institute pediatric circulatory support program: a summary of the 5-year experience. Circulation. 2011;123:1233–40.
141. Addonizio LJ. Pediatric ventricular assist devices—first steps for babies. N Engl J Med. 2012;367:567–8.
142. Romano P, Mangion JM. The role of intraoperative transesophageal echocardiography in heart transplantation. Echocardiography. 2002;19:599–604.
143. Ishizuka N, Nakamura K, Fujita Y, et al. Transesophageal echocardiographic findings in patients after heart transplantation. J Cardiol. 1997;29:163–70.
144. del Rio MJ. Transplantation in complex congenital heart disease. Prog Pediatr Cardiol. 2000;11:107–13.
145. Kirklin JK, Naftel DC, Kirklin JW, Blackstone EH, White-Williams C, Bourge RC. Pulmonary vascular resistance and the risk of heart transplantation. J Heart Transplant. 1988;7:331–6.
146. Meyers BF, Lynch J, Trulock EP, Guthrie TJ, Cooper JD, Patterson GA. Lung transplantation: a decade of experience. Ann Surg. 1999;230:362–70; discussion 370–1.
147. Serra E, Feltracco P, Barbieri S, Forti A, Ori C. Transesophageal echocardiography during lung transplantation. Transplant Proc. 2007;39:1981–2.
148. Hausmann D, Daniel WG, Mugge A, et al. Imaging of pulmonary artery and vein anastomoses by transesophageal echocardiography after lung transplantation. Circulation. 1992;86:II251–8.
149. Gonzalez-Fernandez C, Gonzalez-Castro A, Rodriguez-Borregan JC, et al. Pulmonary venous obstruction after lung transplantation. Diagnostic advantages of transesophageal echocardiography. Clin Transplant. 2009;23:975–80.
150. McIlroy DR, Sesto AC, Buckland MR. Pulmonary vein thrombosis, lung transplantation, and intraoperative transesophageal echocardiography. J Cardiothorac Vasc Anesth. 2006;20:712–5.
151. Asfoura JY, Vidt DG. Acute aortic dissection. Chest. 1991;99:724–9.
152. Flachskampf FA, Daniel WG. Aortic dissection. In: Foster E, editor. Cardiology Clinics: Transesophageal Echocardiography. 18(4) ed. Medizinische Klinik II, Universitat Erlangen-Nurnberg, Germany. frank.flachskampf@rzmail.uni-erlangen.de: United States; 2000. p. 807–17.
153. Nienaber CA, Spielmann RP, von Kodolitsch Y, et al. Diagnosis of thoracic aortic dissection. Magnetic resonance imaging versus transesophageal echocardiography. Circulation. 1992;85:434–47.
154. Matura LA, Ho VB, Rosing DR, Bondy CA. Aortic dilatation and dissection in Turner syndrome. Circulation. 2007;116:1663–70.
155. Erbel R, Bednarczyk I, Pop T, et al. Detection of dissection of the aortic intima and media after angioplasty of coarctation of the aorta. An angiographic, computer tomographic, and echocardiographic comparative study. Circulation. 1990;81:805–14.
156. Kouchoukos NT, Blackstone EH, Hanley FL, Doty DB, Karp RB. Acute aortic dissection. In: Kirklin/Barratt-Boyes cardiac surgery. 3rd ed. Philadelphia: Churchill Livingstone; 2003. p. 1820–49.
157. Miller DC, Mitchell RS, Oyer PE, Stinson EB, Jamieson SW, Shumway NE. Independent determinants of operative mortality for patients with aortic dissections. Circulation. 1984;70:I153–64.
158. DeBakey ME, McCollum CH, Crawford ES, et al. Dissection and dissecting aneurysms of the aorta: twenty-year follow-up of five hundred twenty-seven patients treated surgically. Surgery. 1982;92:1118–34.
159. Keren A, Kim CB, Hu BS, et al. Accuracy of biplane and multiplane transesophageal echocardiography in diagnosis of typical acute aortic dissection and intramural hematoma. J Am Coll Cardiol. 1996;28:627–36.
160. Penco M, Paparoni S, Dagianti A, et al. Usefulness of transesophageal echocardiography in the assessment of aortic dissection. Am J Cardiol. 2000;86:53G–6.
161. Thrumurthy SG, Karthikesalingam A, Patterson BO, Holt PJE, Thompson MM. The diagnosis and management of aortic dissection. BMJ. 2012;344:d8290.